

# Synthesis and Luminescent Properties of Lewis Base-Appended Borafluorenes

Christopher J. Berger, Gang He, Christian Merten, Robert McDonald, Michael J. Ferguson, and Eric Rivard\*

Department of Chemistry, University of Alberta, 11227 Saskatchewan Drive, Edmonton, Alberta, Canada T6G 2G2

## S Supporting Information

**ABSTRACT:** A series of Lewis base adducts of 9-bromo-9-borafluorene (BrBFL-LB, LB = IPr, IPrCH<sub>2</sub>, PPh<sub>3</sub>, and PCy<sub>3</sub>), parent borafluorenes (HBFL-IPr and HBFL-IPrCH<sub>2</sub>), and the bisadduct [(DMAP)<sub>2</sub>BFL]Br were prepared and structurally characterized (IPr = [(HCNDipp)<sub>2</sub>C:], IPrCH<sub>2</sub> = [(HCNDipp)<sub>2</sub>C=CH<sub>2</sub>], Dipp = 2,6-*i*-Pr<sub>2</sub>C<sub>6</sub>H<sub>3</sub>, and DMAP = *N,N*-dimethylaminopyridine). The adducts BrBFL-IPr, BrBFL-PPh<sub>3</sub>, BrBFL-PCy<sub>3</sub>, [(DMAP)<sub>2</sub>BFL]Br, BrBFL-IPrCH<sub>2</sub>, and HBFL-IPrCH<sub>2</sub> were found to exhibit bright blue luminescence with low to moderately high quantum efficiencies (19 to 63%). Selective irradiation at different excitation wavelengths revealed the presence of two distinct emission processes in the adducts BrBFL-LB, leading to a ligand-independent, presumably borafluorene-based, blue light emission at 435 nm and another less intense emission band in the ultraviolet region (315–324 nm); [(DMAP)<sub>2</sub>BFL]Br exhibits an emission profile that tails into the visible region. Time-dependent density functional theory studies are also included for representative borafluorene adducts. With a judicious choice of functional groups at boron, one can envisage the future generation of a whole library of 4-coordinate borafluorene-based luminogens that complement the efficient light-emitting behavior known for the widely studied boron-dipyrromethene analogues.



## INTRODUCTION

The generation of light-emitting materials based upon boron represents a widely explored concept in modern main-group chemistry.<sup>1</sup> One common approach in this field is to fuse low-coordinate boron environments (BR<sub>3</sub>) with organic  $\pi$  frameworks to encourage electronic communication/charge-transfer involving accessible empty p orbitals at boron, leading to fluorescent behavior.

Of particular relevance to the current study, Wagner and co-workers have developed light-emitting diboraanthracenes (Figure 1),<sup>2,3</sup> while luminescent materials based on borafluorene scaffolds have been reported by Yamaguchi and co-

workers.<sup>4</sup> In addition the Jäkle group has successfully incorporated 3-coordinate boron environments within oligomeric and polymeric arrays for fluorescence-based sensing applications (Figure 1).<sup>5</sup> In general, sterically encumbered substituents (e.g., Trip; Trip = 2,4,6-*i*-Pr<sub>3</sub>C<sub>6</sub>H<sub>2</sub>) are required at boron to render the materials stable to oxygen and water, while concurrently enabling the p orbitals at boron to remain accessible for electronic interactions leading to luminescence. In this Paper we report new, well-defined borafluorene-based emitters containing 4-coordinate environments.<sup>1c</sup> These species display photoluminescence in the visible spectral region and can be considered to be molecular analogues to the well-documented boron-dipyrromethene (BODIPY) class of emitters (Figure 1).<sup>1a,b</sup>

## RESULTS AND DISCUSSION

**Preparation of Lewis Base Adducts of 9-Bromo-9-borafluorene (BrBFL).** The central structural motif of the compounds reported in this paper is the planar borafluorene array (abbreviated as BFL hereafter). We initially prepared the haloborafluorene 9-bromo-9-borafluorene BrBFL (1) as a potential synthon to access boron-containing polymers but soon uncovered that coordination of this Lewis acidic species with electron pair donors afforded adducts with bright blue luminescence when irradiated with UV light (*vide infra*).

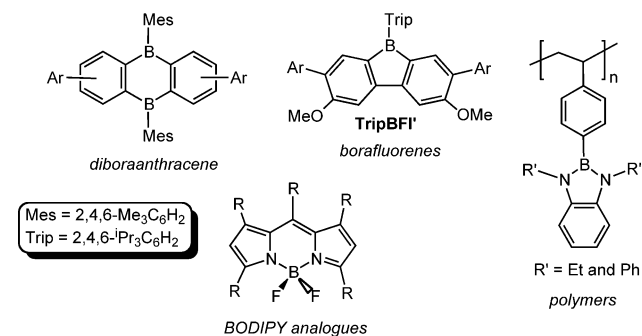
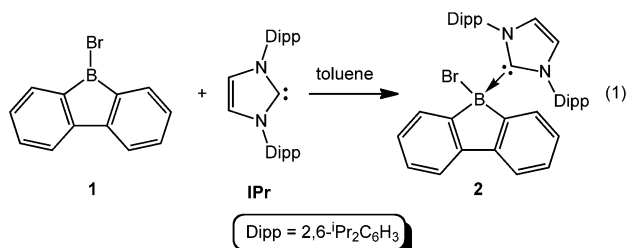


**Figure 1.** Selected examples of light-emitting materials containing boron.

Received: September 23, 2013

Published: January 15, 2014

The first molecular BrBFl adduct prepared in our study BrBFl–IPr (**2**) was obtained by combining the Lewis base IPr (IPr = [(HCNDipp)<sub>2</sub>C:]<sup>-</sup>; Dipp = 2,6-*i*-Pr<sub>2</sub>C<sub>6</sub>H<sub>3</sub>) with **1** in toluene (eq 1). Isolation of BrBFl–IPr (**2**) in high purity and



yield is straightforward as compound **2** is only sparingly soluble in toluene and thus precipitates as it is formed in the reaction mixture. This Lewis base coordinated borafluorene is a colorless solid, and comprehensive characterization of this species was achieved by a combination of NMR spectroscopy, single-crystal X-ray crystallography (Figure 2), and elemental analysis. The

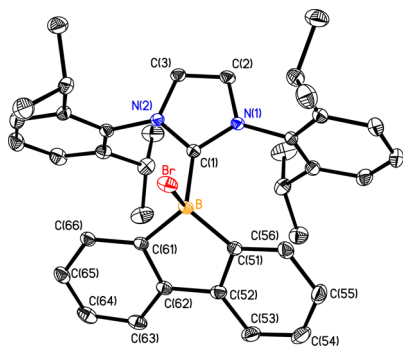


**Figure 2.** Thermal ellipsoid plot (30% probability) of BrBFl–IPr (**2**) with hydrogen atoms and CH<sub>2</sub>Cl<sub>2</sub> solvate molecules omitted for clarity. Selected bond lengths (Å) and angles (deg): B–Br 2.114(2), B–C(1) 1.639(3), B–C(51) 1.619(3), B–C(61) 1.619(3); Br–B–C(1) 101.47(13), Br–B–C(51) 108.32(14), Br–B–C(61) 111.65(14), C(51)–B–C(61) 110.14(17), C(1)–B–C(51) 119.11(18), C(1)–B–C(61) 116.27(17).

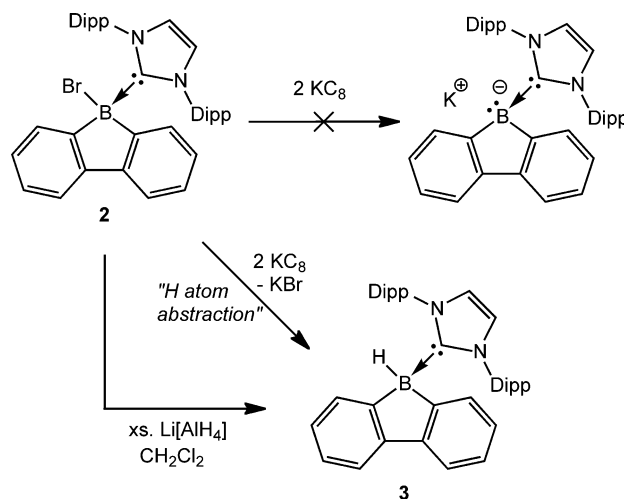
presence of a coordinated IPr unit in **2** is evident from the <sup>1</sup>H and <sup>13</sup>C{<sup>1</sup>H} NMR spectra, while a <sup>11</sup>B NMR resonance belonging to **2** appears at –6.4 ppm. This latter resonance is in line with the presence of a 4-coordinate boron environment, and this signal is positioned significantly upfield in relation to the resonance found in the 3-coordinate borafluorene **1** ( $\delta$  65.8 ppm).<sup>6</sup> BrBFl–IPr (**2**) is remarkably stable, with no visible decomposition or melting noted up to 340 °C in the solid state under a nitrogen atmosphere. Moreover, unlike **1**, compound **2** is moisture-stable as the addition of H<sub>2</sub>O to a solution of **2** in CDCl<sub>3</sub> did not result in any discernible hydrolysis. In addition, compound **2** yields bright blue luminescence when irradiated in CH<sub>2</sub>Cl<sub>2</sub> at 252 nm, and this effect (and the photoluminescence from related BrBFl–LB adducts; LB = Lewis base) will be discussed in detail later in this paper.

As anticipated from the spectral data, compound **2** contains a 4-coordinate environment about boron (Figure 2) with a concomitantly longer B–Br bond length [2.114(2) Å] in comparison to that found in BrBFl (**1**) [1.909(10) Å].<sup>7</sup> In addition the intraring B–C(borafluorene) distances in **2** [1.619(3) Å average] are expanded by ca. 0.1 Å relative to the B–C endocyclic bond lengths found within the donor-free

borafluorene **1**. The exocyclic B–C<sub>IPr</sub> interaction in **2** is 1.639(3) Å and is of similar value to the dative B–C interactions within known carbene adducts of heterocyclic boron species in the literature, including the tetraphenylborole adduct BrBC<sub>4</sub>Ph<sub>4</sub>–SIMes (1.655(3) Å; SIMes = [(H<sub>2</sub>CNMe)<sub>2</sub>C:]<sup>-</sup>).<sup>8</sup>

Intrigued by the isolation of a carbene-supported anionic boryl heterocycle K[SIMes–BC<sub>4</sub>Ph<sub>4</sub>] by Braunschweig and co-workers, we attempted to prepare an analogous carbene-bound borafluorene.<sup>8b</sup> The ultimate goal was to use the resulting nucleophilic boron center to access new borafluorene analogues with novel optoelectronic properties. In pursuit of this goal, we combined **2** with 2 equiv of potassium graphite (KC<sub>8</sub>) in diethyl ether. A new, upfield-shifted, <sup>11</sup>B{<sup>1</sup>H} NMR resonance was noted at –19.1 ppm when the reaction mixture was analyzed; however, this signal split into a doublet in the proton-coupled <sup>11</sup>B NMR spectrum (<sup>1</sup>J<sub>BH</sub> = 84 Hz), indicating the presence of a B–H group in the final product. Multiple attempts to reduce **2** with KC<sub>8</sub> under different conditions in tetrahydrofuran (THF) and toluene (–78 °C to room temperature) gave the same boron-containing product. Treatment of **2** with the milder reducing agents Na(s), sodium naphthalenide, and 5% Na(Hg) amalgam in THF gave no reaction. Positing that the product formed was the hydridoborane adduct HBFl–IPr (**3**), we reacted **2** with the hydride source Li[AlH<sub>4</sub>] (Scheme 1). As expected, the resulting

#### Scheme 1. Generation of the Donor-Stabilized Parent Borafluorene HBFl–IPr via Treatment of BrBFl–IPr with Either KC<sub>8</sub> or Li[AlH<sub>4</sub>]



product obtained after crystallization (27% yield) was the colorless solid HBFl–IPr (**3**). This compound gave identical spectroscopic features as the product obtained between the reaction of **2** with KC<sub>8</sub>, including a doublet resonance at –19.1 ppm in the <sup>11</sup>B NMR spectrum; thus, it appears that the target borafluorene anion [IPr–BFl]<sup>-</sup> is unstable under the reaction conditions explored and undergoes hydrogen abstraction chemistry either with the solvent or with residual water. Crystals of **3** suitable for X-ray analysis were grown from a mixture of CH<sub>2</sub>Cl<sub>2</sub> and hexanes at –35 °C, and the refined structure is presented in Figure 3.

The metrical parameters within the borafluorene (BFl) unit in HBFl–IPr (**3**) are similar to those found in the bromo adduct **2**, while the dative B–C<sub>IPr</sub> bond length in **3**, 1.6232(17)

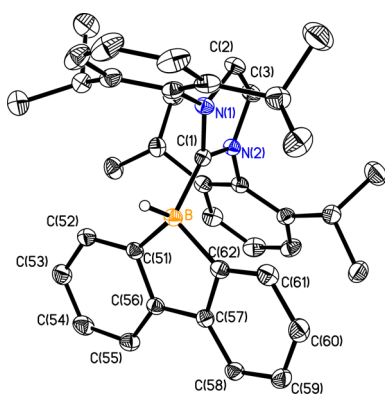
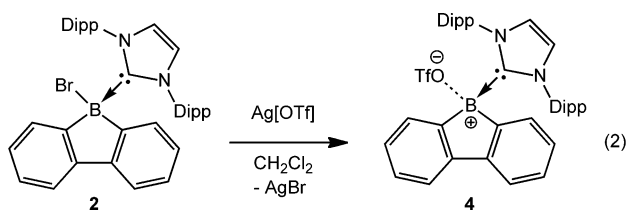


**Figure 3.** Thermal ellipsoid plot (30% probability) of HBfI-IPr (**3**) with the carbon-bound hydrogen atoms omitted for clarity. Selected bond lengths (Å) and angles (deg): B–H(1B) 1.135(14), B–C(1) 1.6232(16), B–C(51) 1.6232(17), B–C(62) 1.6258(17); H(1B)–B–C(1) 105.8(7), H(1B)–B–C(51) 109.4(7), Br–B–C(62) 110.6(7), C(51)–B–C(62) 99.31(9), C(1)–B–C(51) 117.85(9), C(1)–B–C(62) 113.80(9).

Å, is only slightly shorter than the corresponding distance in **2**. The major difference in the structures of both adducts is that the IPr unit of **3** is twisted by approximately 90° about the boron-carbene carbon bond relative to that in **2**; as a result, one of the flanking Dipp groups within the IPr donor in **3** is positioned above the B–H bond vector. The hydrogen atom at boron was located in the electron difference map and isotropically refined to yield a B–H bond length of 1.135(14) Å. The related base-stabilized borafluorenes<sup>9</sup> Me<sub>2</sub>S–HBfI<sup>9a</sup> and *t*-Bu<sub>2</sub>PH–HBfI<sup>9c</sup> were recently characterized by X-ray crystallography, and these species have similar overall geometric arrangements as in **3**.

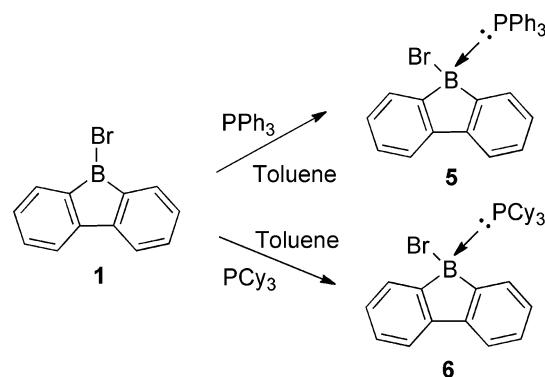
We also investigated the formation of a base-stabilized borafluorenium cation.<sup>10</sup> When an equimolar ratio of Ag[OTf] (OTf = triflate, F<sub>3</sub>CSO<sub>3</sub><sup>−</sup>) and BrBfI–IPr (**2**) were allowed to react in CH<sub>2</sub>Cl<sub>2</sub>, the triflate-substituted borafluorene (TfO)–BfI–IPr (**4**) was isolated as a colorless solid in a 45% yield (eq 2). <sup>11</sup>B NMR spectroscopy (CDCl<sub>3</sub>) yields a singlet resonance



at 2.3 ppm that is slightly downfield-positioned relative to the <sup>11</sup>B NMR resonance observed for **2**. The OTf group in **4** resonates at −77.8 ppm in the <sup>19</sup>F NMR spectrum and is consistent with the presence of a coordinated OTf group at boron; for comparison the free OTf<sup>−</sup> anion in [*n*-Bu<sub>4</sub>N][OTf] gives a <sup>19</sup>F NMR resonance at −78.7 ppm.<sup>11</sup> In addition rigorously 3-coordinate borenium cations typically have <sup>11</sup>B NMR chemical shifts >20 ppm,<sup>12</sup> adding further support for a boron-bound OTf group in **4**. Unfortunately our attempts to grow X-ray quality crystals of **4** where not successful; but, satisfactory elemental analyses (C, H, and N) were obtained, and a molecular ion for [(TfO)BfI–IPr]<sup>+</sup> was detected by mass spectrometry. Attempts to reduce the borafluorene center in **4** with KC<sub>8</sub> invariably led to the formation of the hydridoborafluorene adduct HBfI–IPr (**3**) as evidenced by <sup>1</sup>H and <sup>11</sup>B

NMR spectroscopy. It is salient to mention that a cationic borafluorene was successfully prepared by Narula and Nöth in the form of the acridine adduct [(acridine)BfI]AlCl<sub>4</sub>.<sup>13</sup> With the intention of expanding the scope of coordination chemistry involving BrBfI (**1**), this borafluorene was combined with triphenylphosphine, tricyclohexylphosphine, and *N,N*-dimethylaminopyridine (DMAP) donors, respectively. The synthesis of the triphenylphosphine adduct of **1**, BrBfI–PPh<sub>3</sub> (**5**), proceeded in a similar fashion as the *N*-heterocyclic carbene analogue **2** by combining a 1:1 mixture of **1** and PPh<sub>3</sub> in toluene (Scheme 2). The sparingly soluble phosphine complex

**Scheme 2. Preparation of the Triphenylphosphine- and Tricyclohexylphosphine-Substituted Borafluorene Adducts BrBfI–PPh<sub>3</sub> (**5**) and BrBfI–PCy<sub>3</sub> (**6**)**



BrBfI–PPh<sub>3</sub> (**5**) was isolated in a 92% yield. The <sup>1</sup>H and <sup>13</sup>C{<sup>1</sup>H} NMR spectra of **5** in CDCl<sub>3</sub> gave expected resonances for the borafluorene and PPh<sub>3</sub> units, while a 4-coordinate boron environment was identified by <sup>11</sup>B NMR spectroscopy (δ −7.4 (br)); no discernible P–B coupling was observed, likely due to low symmetry present at boron, leading to increased quadrupolar broadening of the resonance. The <sup>31</sup>P NMR resonance of **5** (δ 1.8) is shifted slightly downfield from the resonance due to free PPh<sub>3</sub> (δ −5.3). Repeated attempts to grow crystals suitable for X-ray analysis were unsuccessful; however, additional confirmation for the formation of **5** was provided through mass spectrometry and elemental analysis. The synthesis of the related tricyclohexylphosphine adduct BrBfI–PCy<sub>3</sub> (**6**) proceeded in a similar manner as **5**, leading to the formation of **6** as an analytically pure colorless solid in a 87% yield. As will be detailed later, compounds **5** and **6** display similar bright blue luminescence as **2** (vide infra).

Divergent chemistry transpired between DMAP and BrBfI (**1**) with respect to what was noted for Ph<sub>3</sub>P, IPr, and PCy<sub>3</sub>. Treatment of **1** with 1 equiv of DMAP in toluene gave a crude reaction mixture with a new DMAP-containing product (by <sup>1</sup>H and <sup>13</sup>C{<sup>1</sup>H} NMR spectroscopy); however, a significant quantity of unreacted **1** was also present. By increasing the amount of DMAP relative to boron in the reaction mixture to a molar ratio of 2:1, the previously observed product formed in a much higher yield and could be readily isolated in pure form as a colorless solid. NMR spectroscopy identified the presence of **2** equiv of DMAP relative to the BrBfI unit, while a 4-coordinate boron environment with an upfield-shifted resonance (relative to free **1**) was detected at 4.6 ppm by <sup>11</sup>B NMR spectroscopy. X-ray crystallography performed on crystals grown from a mixture of THF and CH<sub>2</sub>Cl<sub>2</sub> at −35 °C corroborated the incorporation of two DMAP donors at boron

to give the borafluorenum salt  $[(\text{DMAP})_2\text{BFl}]\text{Br}$  (**7**) with a distorted tetrahedral geometry at boron (Figure 4). To be

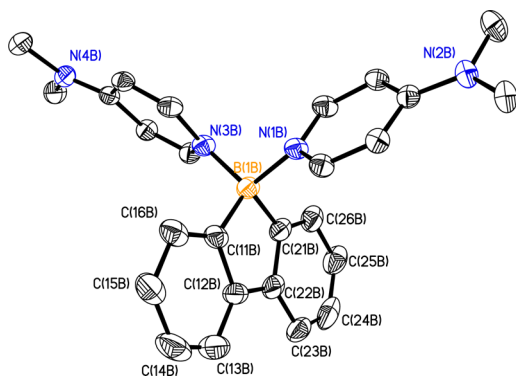
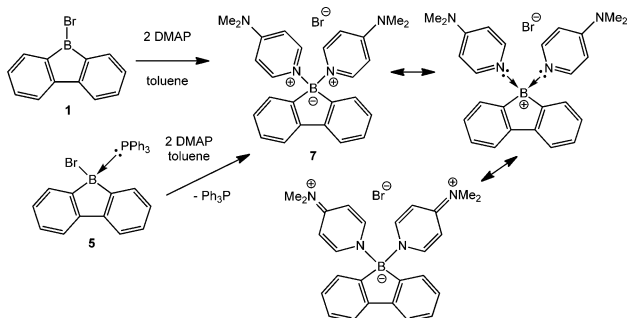


**Figure 4.** Thermal ellipsoid plot (30% probability) of  $[(\text{DMAP})_2\text{BFl}]\text{Br}$  (**7**) with hydrogen atoms, bromide anion, and  $\text{CH}_2\text{Cl}_2$  solvate molecules omitted for clarity. Three molecules of **7** are present in the asymmetric unit; thus, only one of these molecules is presented above. Selected bond lengths (Å) and angles (deg) with values for the two other molecules in the asymmetric unit in square brackets: B(1B)–N(1B) 1.582(5) [1.584(5), 1.576(5)], B(1B)–N(3B) 1.582(5) [1.597(5), 1.604(5)], B(1B)–C(11B) 1.609(6) [1.606(6), 1.620(6)], B(1B)–C(21B) 1.632(6) [1.606(6), 1.629(6)]; N(1B)–B(1B)–N(3B) 108.2(3) [105.8(3), 102.2(4)], C(11B)–B(1B)–C(21B) 100.6(3) [100.8(3), 100.2(3)], N(1B)–B(1B)–C(11B) 112.6(3) [114.0(3), 110.2(3)], N(1B)–B(1B)–C(21B) 108.6(3) [110.8(3), 113.4(3)], N(3B)–B(1B)–C(11B) 111.8(3) [112.5(4), 114.3(4)], N(3B)–B(1B)–C(21B) 115.0(3) [113.0(3), 109.0(5)].

discussed in more detail later, compound **7** is also photoluminescent in solution. Furthermore, the  $\text{PPh}_3$  donor in  $\text{BrBFl}-\text{PPh}_3$  (**5**) can be readily displaced by 2 equiv of DMAP to generate  $[(\text{DMAP})_2\text{BFl}]\text{Br}$  (**7**) and free  $\text{PPh}_3$  in a quantitative fashion (Scheme 3).

### Scheme 3. Preparation of the Doubly Substituted Borafluorene-DMAP Adduct, $[(\text{DMAP})_2\text{BFl}]\text{Br}$ (**7**)

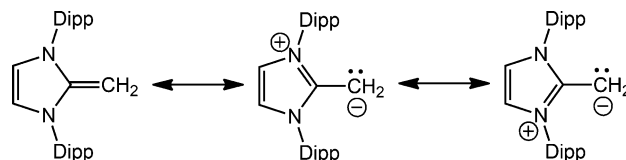


The boron–carbon bond distances within the borafluorene unit in **7** are the same within experimental error as those seen in  $\text{BrBFl}-\text{IPr}$  (**2**) and  $\text{HBFl}-\text{IPr}$  (**3**) (Figures 2 and 3). The boron–nitrogen bond distances in **7** range from 1.576(5) to 1.604(5) Å and are similar to the reported pyridine–borafluorene N–B bond lengths found in the literature; specifically, the *t*-Bu-substituted hydridoborafluorene adduct  $[2,7\text{-}t\text{-Bu}_2\text{C}_6\text{H}_6\text{BH}-\text{pyridine}]^{\text{9b}}$  has a dative B–N bond length of 1.564(5) Å, while the azidoborafluorene complex  $\text{N}_3\text{BFl}-\text{pyridine}$ <sup>14</sup> has a B–N distance of 1.619(2) Å. Interestingly the B–N distance within Nöth's acridine borafluorenum adduct  $[(\text{acridine})\text{BFl}]^+$  is slightly elongated relative to **7** [1.650(11)

Å] despite the presence of a 3-coordinate boron center in  $[(\text{acridine})\text{BFl}]^+$ ;<sup>13</sup> this effect highlights the strong donating ability of DMAP.

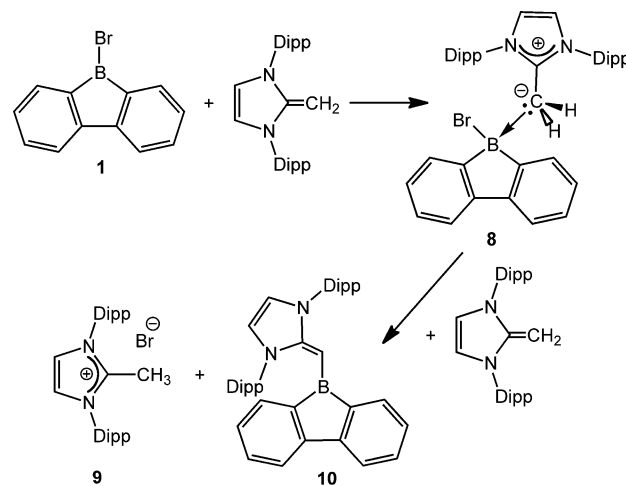
Hoping to isolate an additional borafluorene adduct with luminescent properties, attention turned to the use of the *N*-heterocyclic olefin (NHO),  $\text{IPrCH}_2$  ( $\text{IPrCH}_2 = (\text{HCNDipp})_2\text{C}=\text{CH}_2$ ) as a Lewis base. Note that  $\text{IPrCH}_2$  has been used as a donor ligand in *p*-block chemistry,<sup>15,16</sup> and the nucleophilic/ylidic character of the terminal  $\text{CH}_2$  group is described by the canonical forms illustrated in Scheme 4.<sup>17</sup>

### Scheme 4. Representative Canonical Forms for $\text{IPrCH}_2$



The direct reaction of  $\text{IPrCH}_2$  with  $\text{BrBFl}$  (**1**) progressed in a somewhat complex fashion, necessitating considerable optimization of the reaction conditions to generate the target adduct  $\text{BrBFl}-\text{IPrCH}_2$  (**8**) in high yield. When  $\text{IPrCH}_2$  and **1** were allowed to react in a 1:1 molar ratio in toluene, a white precipitate formed that contained  $\text{BrBFl}-\text{IPrCH}_2$  (**8**) (vide infra) and the methylimidazolium salt  $[\text{IPrMe}]\text{Br}$  (**9**);<sup>18</sup> the latter species was prepared independently by bubbling  $\text{HBr}$  gas through a solution of  $\text{IPrCH}_2$  in toluene. The soluble fraction from the reaction of  $\text{IPrCH}_2$  and **1** contained unreacted starting materials along with a new boron-containing product (<sup>11</sup>B NMR resonance at 2.6 ppm). This product has been tentatively assigned as the vinyl-substituted borafluorene  $(\text{IPr}=\text{CH})\text{BFl}$  (**10**)<sup>19</sup> and would form via the  $\text{IPrCH}_2$ -induced deprotonation of **8**, leading to the generation of the  $[\text{IPrMe}]\text{Br}$  coproduct observed; related chemistry has been reported recently in our group.<sup>15b</sup> Thus far, attempts to generate **10** in a definitive fashion by reacting **1** with excess  $\text{IPrCH}_2$  have been unsuccessful. Fortunately, if the ratio between **1** and  $\text{IPrCH}_2$  is kept at 2:1 (i.e., excess **1** according to Scheme 5), then sparingly soluble  $\text{BrBFl}-\text{IPrCH}_2$  (**8**) can be recovered from toluene in a nearly quantitative fashion. Compound **8** gives a <sup>11</sup>B NMR resonance at 1.4 ppm, while the methylene  $\text{CH}_2$  protons within the  $\text{IPrCH}_2$  donor resonate at 2.66 ppm

### Scheme 5. Synthesis of $\text{BrBFl}-\text{IPrCH}_2$ (**8**)



(CDCl<sub>3</sub>) in the <sup>1</sup>H NMR spectrum. For comparison, the IPrCH<sub>2</sub> aminoborane adduct IPrCH<sub>2</sub>-BH<sub>2</sub>NMe<sub>2</sub>BH<sub>3</sub> has a CH<sub>2</sub> resonance at 1.96 ppm (CDCl<sub>3</sub>). Structural authentication of **8** was provided by single-crystal X-ray diffraction, and the refined structure is presented in Figure 5.

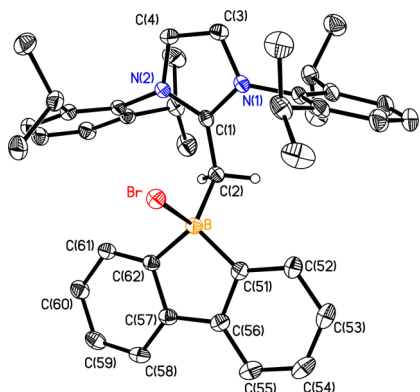
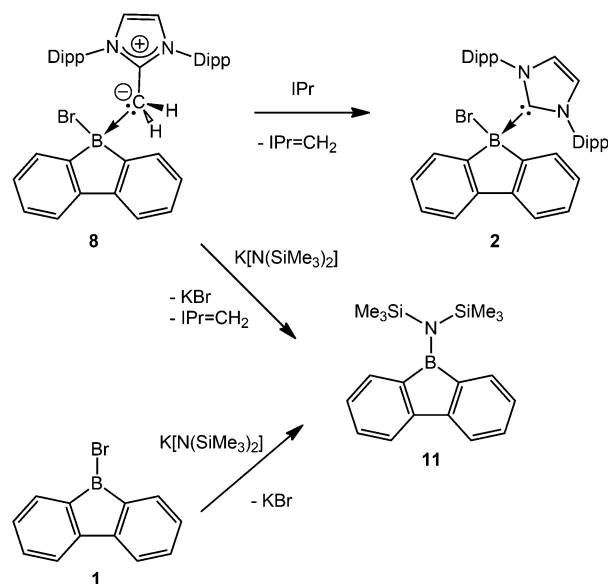


**Figure 5.** Thermal ellipsoid plot (30% probability) of BrBFI-IPrCH<sub>2</sub> (**8**) with all hydrogen atoms, except those at C(2), and CH<sub>2</sub>Cl<sub>2</sub> solvate molecules omitted for clarity. Selected bond lengths (Å) and angles (deg): B-Br 2.124(2), B-C(2) 1.660(3), B-C(51) 1.609(3), B-C(62) 1.610(3), C(1)-C(2) 1.473(2); C(51)-B-C(62) 100.29(15), C(51)-B-Br 106.29(12), C(62)-B-Br 106.94(13), C(51)-B-C(2) 115.38(16), C(62)-B-C(2) 116.19(15), Br-B-C(2) 110.75(12), B-C(1)-C(2) 121.83(15).

As noted previously, the metrical parameters within the borafluorene (BFI) units are rather insensitive to the nature of the Lewis base(s) coordinated to boron. The B-CH<sub>2</sub> bond length in BrBFI-IPrCH<sub>2</sub> (**8**) (1.660(3) Å) is slightly elongated compared to the analogous B-C<sub>IPr</sub> bond in **2** (1.639(3) Å), and is similar in value to the corresponding bond lengths in the IPrCH<sub>2</sub>-borane adducts prepared in our group (e.g., B-C bond length of 1.659(3) Å in IPrCH<sub>2</sub>-H<sub>2</sub>BNMe<sub>2</sub>-BH<sub>3</sub>).<sup>15c</sup> The C(1)-C(2) bond length within the IPrCH<sub>2</sub> donor in **8** [1.473(2) Å] approaches the length expected for a carbon-carbon single bond (approximately 1.54 Å), indicating that  $\pi$  electron density in IPr=CH<sub>2</sub> is being drawn away to form a new B-C coordinative bond in **8**; for comparison, the related carbon-carbon distance in free IPrCH<sub>2</sub> is 1.331(8) Å (average).<sup>20</sup>

Attempts were made to eliminate HBr from **8** to form the alkenyl-substituted borafluorene (IPr=CH)BFI **10**. When the potential Brønsted base, IPr, was combined with **8**, it was discovered that IPr had exchanged with IPrCH<sub>2</sub> at boron, resulting in the formation of BrBFI-IPr (**2**) and free IPrCH<sub>2</sub> (Scheme 6). This observation is in line with previous chemistry from our group illustrating that IPrCH<sub>2</sub> is a weaker donor than IPr.<sup>15a,c</sup> Addition of the weakly nucleophilic base K[N(SiMe<sub>3</sub>)<sub>2</sub>] to **8** gave a new boron-containing product and free IPrCH<sub>2</sub> in the crude reaction mixture (by <sup>1</sup>H and <sup>11</sup>B NMR spectroscopy). The new product had a <sup>11</sup>B NMR resonance at 54.2 ppm (in CDCl<sub>3</sub>), which strongly suggested the presence of a 3-coordinate boron center. Given that well-defined <sup>1</sup>H, <sup>13</sup>C{<sup>1</sup>H}, and <sup>29</sup>Si{<sup>1</sup>H} resonances were present for both the borafluorene and N(SiMe<sub>3</sub>)<sub>2</sub> moieties, the product (red semisolid) was formulated as the amidoborafluorene FIB[N(SiMe<sub>3</sub>)<sub>2</sub>] (**11**).<sup>18</sup> Furthermore, this product can be prepared from the direct reaction of K[N(SiMe<sub>3</sub>)<sub>2</sub>] with BrBFI **1** (Scheme 6). These results show that the presence of a sterically encumbered and

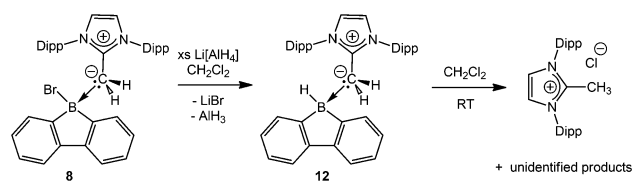
### Scheme 6. Formation of the Amidoborafluorene FIB[N(SiMe<sub>3</sub>)<sub>2</sub>] (**11**) by Two Different Routes



potentially  $\pi$ -donating -N(SiMe<sub>3</sub>)<sub>2</sub> group at boron in **11** reduces the electrophilicity (and Lewis acidity) of the borafluorene unit, preventing coordination of IPrCH<sub>2</sub> from transpiring.

Drawing inspiration from the successful synthesis of HBFI-IPr via Br/H exchange (Scheme 1), we prepared the nucleophilic olefin-capped borafluorene HBFI-IPrCH<sub>2</sub> (**12**) by combining BrBFI-IPrCH<sub>2</sub> (**8**) with an excess of Li[AlH<sub>4</sub>] in CH<sub>2</sub>Cl<sub>2</sub> (Scheme 7). Proton-coupled <sup>11</sup>B NMR spectroscopy

### Scheme 7. Synthesis of the IPrCH<sub>2</sub>-Capped Parent Borafluorene Adduct HBFI-IPrCH<sub>2</sub> (**12**) and Instability of This Species in Solution



identified the presence of a B-H unit (doublet at -15.1; <sup>1</sup>J<sub>BH</sub> = 82 Hz), while spectral features for the remaining borafluorene unit were identifiable by <sup>1</sup>H, <sup>11</sup>B, and <sup>13</sup>C{<sup>1</sup>H} NMR spectroscopy. Attempts to grow crystals suitable for X-ray analysis from a mixture of CH<sub>2</sub>Cl<sub>2</sub> and hexanes exclusively gave the known salt [IPrMe]Cl<sup>15b</sup> as a crystalline product. To verify if HBFI-IPrCH<sub>2</sub> (**12**) was decomposing during the above-mentioned crystallization attempts, a solution of **12** in CH<sub>2</sub>Cl<sub>2</sub> was stirred for 3 d in the absence of Li[AlH<sub>4</sub>]. Analysis of this product showed that the [IPrMe]Cl salt was present (ca. 70% by <sup>1</sup>H NMR), along with several unidentified boron-containing compounds. Elemental analyses on **12** routinely gave low values for carbon; thus, copies of the NMR spectra for **12** have been deposited as part of the Supporting Information.<sup>18</sup>

**Photophysical Properties of BrBFI-IPr (2), BrBFI-PPh<sub>3</sub> (5), BrBFI-PCy<sub>3</sub> (6), [(DMAP)<sub>2</sub>BFI]Br (7), BrBFI-IPrCH<sub>2</sub> (8), and HBFI-IPrCH<sub>2</sub> (12).** As stated earlier, the adducts in this study, BrBFI-IPr (**2**), BrBFI-PPh<sub>3</sub> (**5**), BrBFI-PCy<sub>3</sub> (**6**), [(DMAP)<sub>2</sub>BFI]Br (**7**), and XBFI-IPrCH<sub>2</sub> (X = Br and H; **8**

and 12), exhibit bright blue luminescence in halogenated solvents when irradiated with ultraviolet (UV) light ( $\lambda_{\text{excit.}} = 252$  nm for compounds 2, 5, 6, 8, and 12;  $\lambda_{\text{excit.}} = 320$  nm for compound 7). Figures 6 and 7 show the ultraviolet–visible

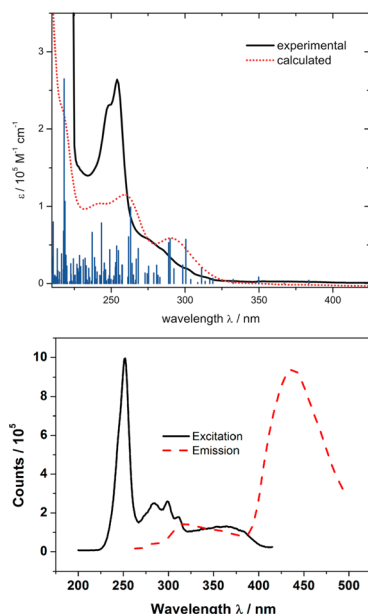


**Figure 6.** (top panel) UV–vis absorbance spectrum (solid line) of BrBFl–PPh<sub>3</sub> (5) in CH<sub>2</sub>Cl<sub>2</sub>, with the calculated spectrum (dotted line) as derived from TD–DFT. The calculated line spectrum reflecting the oscillator strengths for the various transitions present is also shown. (bottom panel) Fluorescence excitation (dashed line) and emission spectrum (solid line) for compound 5.  $\lambda_{\text{excit.}} = 252$  nm.

(UV–vis) absorbance and fluorescence excitation/emission spectra for two representative adducts BrBFl–PPh<sub>3</sub> (5) and BrBFl–IPrCH<sub>2</sub> (8), while the related UV–vis and emission data for BrBFl–IPr (2), BrBFl–PCy<sub>3</sub> (6), [(DMAP)<sub>2</sub>BFl]Br (7), and HBFl–IPrCH<sub>2</sub> (12) have been included as part of the Supporting Information.<sup>18</sup> Initially we expected the luminescence in our borafluorene adducts to be quenched due to the lack of a vacant p orbital on boron to participate in conjugation/emission, as noted previously.<sup>3</sup> However after surveying the literature it was noted that Yamaguchi’s borafluorenes TripBFl’ (Figure 1) show blue luminescence when placed in dimethylformamide (DMF) solvent;<sup>4</sup> thus, it now appears that their blue luminescent species could be 4-coordinate borafluorene TripBFl’–DMF adducts of similar structure to the BrBFl–LB complexes presented in this Study.<sup>21</sup>

The UV–vis absorbance maxima for compounds 2, 5–8, and 12 each occur between 240 and 290 nm, while tailing of the absorption profile to ca. 300 nm was noted in the BrBFl–LB adducts. The corresponding molar absorptivity coefficients for each major absorbance band were large ( $0.53$ – $2.84 \times 10^3$  M<sup>−1</sup> cm<sup>−1</sup>) and increased with respect to the Lewis base in the order IPr < DMAP < PCy<sub>3</sub> < PPh<sub>3</sub> < IPrCH<sub>2</sub>. Most striking was the presence of nearly identical emission bands at 435 nm for each of the monoadducts (BrBFl–LB) 2, 5, 6, 8, and 12 when irradiated at 252 nm in CH<sub>2</sub>Cl<sub>2</sub>. A second emission band was seen in each complex from 315 to 325 nm that was much less intense than the peak at 435 nm than the peak at 435 nm. The invariant nature of the positions of these emission bands, as the Lewis base (LB) bound at boron is varied, strongly suggests that the fluorescence occurs from the borafluorene unit without

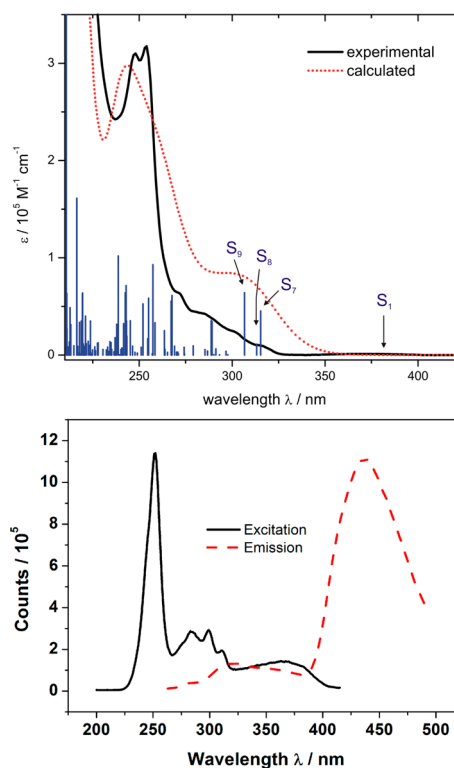


**Figure 7.** (top panel) UV–vis absorbance spectrum (solid line) of BrBFl–IPrCH<sub>2</sub> (8) in CH<sub>2</sub>Cl<sub>2</sub>, with the calculated spectrum (dotted line) as derived from TD–DFT. The calculated line spectrum reflecting the oscillator strengths for the various transitions present is also shown. (bottom panel) Fluorescence excitation (dashed line) and emission spectrum (solid line) for compound 8.  $\lambda_{\text{excit.}} = 252$  nm.

significant participation from the accompanying Lewis basic donors (vide infra).<sup>22</sup> The structurally distinct DMAP complex [(DMAP)<sub>2</sub>BFl]Br (7) also yielded a discernible emission spectra with a maxima of ca. 355 nm ( $\lambda_{\text{excit.}} = 320$  nm) with significant tailing into the violet/blue region (Supporting Information, Figure S11). The quantum yields, measured relative to quinine sulfate in 1 N H<sub>2</sub>SO<sub>4</sub>, were found to be 19, 50, 31, 63, and 19% for BrBFl–IPr (2), BrBFl–PPh<sub>3</sub> (5), BrBFl–PCy<sub>3</sub> (6), BrBFl–IPrCH<sub>2</sub> (8), and HBFl–IPrCH<sub>2</sub> (12), respectively; the fluorescence data for 12 should be interpreted with great caution, as this species consistently contained an unidentifiable impurity, despite repeated recrystallization attempts.<sup>18</sup> The quantum yield of [(DMAP)<sub>2</sub>BFl]Br (7) in DCM is 51%, relative to naphthalene in cyclohexane. These quantum yields were found to be in agreement with those obtained from BODIPY derivatives with 4-coordinate boron centers.<sup>1b,23</sup> To our knowledge, this is the first report of well-defined fluorescent Lewis base–borafluorene adducts, and given that the luminescent compounds contain reactive boron–bromine bonds, functionalization at boron should be possible to generate substituted borafluorenes with potentially tunable light-emitting properties.

The luminescent borafluorene systems reported by Yamaguchi and co-workers have 3-coordinate boron centers leading to significant  $p_{\pi}$ – $\pi^*$  conjugation in the LUMO states involving the vacant p orbital of boron and the  $\pi^*$  manifold of the ancillary biaryl moiety.<sup>4,24</sup> The corresponding HOMO levels are localized on the aromatic C atoms of the borafluorene unit. Upon coordination of an incoming donor species (i.e., F<sup>−</sup> or CN<sup>−</sup>) the delocalization of the LUMO throughout the  $p_{\pi}$ – $\pi^*$

system is disrupted, leading to the emergence of a new fluorescence profile accompanied by a dramatic fluorescence color change.<sup>4</sup> Noting the possible parallel between Yamaguchi's donor-bound borafluorenes and our stable 4-coordinate adducts, we performed TD-DFT studies (B3LYP/6-31G(d,p)) to gain added insight into the electronic transitions involved in the UV–vis spectra of the borafluorene adducts **5**, **7**, and **8** (Figures 7 and 8).

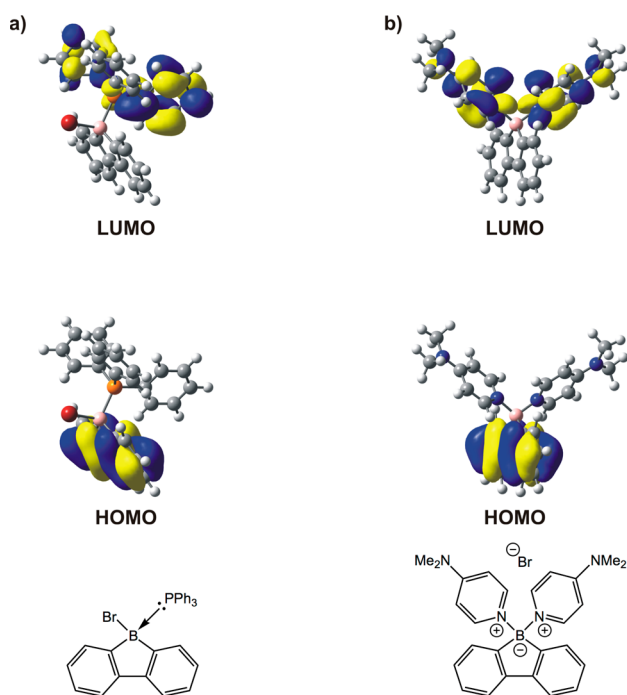


**Figure 8.** Computationally derived HOMO and LUMO plots for (a) BrBFL–PPh<sub>3</sub> (**5**) and (b) [(DMAP)<sub>2</sub>BFL]Br (**7**).

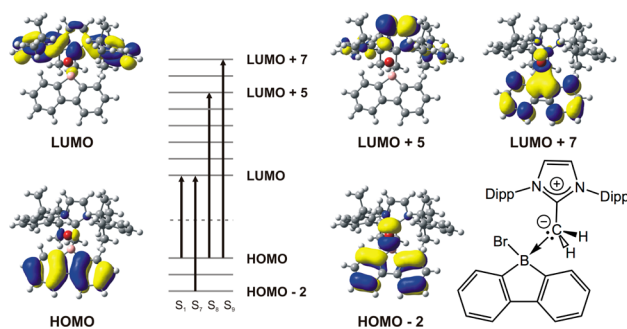


**Figure 9.** Selected electronic transitions computed for BrBFL–IPrCH<sub>2</sub> (**8**); see the Supporting Information for a detailed listing.<sup>18</sup>

The calculated HOMO and LUMO plots for compounds **5**, **7**, and **8** are shown in Figures 8 and 9. In each compound, the HOMO levels were of C–C  $\pi$ -bonding character and located entirely on the borafluorene biaryl units; the LUMO states were exclusively positioned on the Lewis bases and had C–C or C–N  $\pi^*$  character. However, these charge-transfer HOMO–LUMO transitions do not appear to be important in dictating the luminescence of compounds **5**, **7**, and **8**, as the oscillator strengths were found to be zero in all cases (see Supporting Information for a summary of selected calculated electronic transitions computed);<sup>18</sup> thus, the light absorption leading to luminescence involved alternate electronic transitions. Given

that compounds **5** and **8** show nearly identical emission profiles (Figures 7 and 8), despite the presence of distinct PPh<sub>3</sub> and IPrCH<sub>2</sub> donors, respectively, the search for identifiable  $\pi$  to  $\pi^*$  absorptions on the borafluorene units was conducted. As illustrated in Figures 7 and 8, this search was complicated due to the vast numbers of electronic transitions present in BrBFL–PPh<sub>3</sub> (**5**) and BrBFL–IPrCH<sub>2</sub> (**8**), including those that are entirely based on the Lewis basic PPh<sub>3</sub> and IPrCH<sub>2</sub> units and those involving orbital participation from both a BFL unit and the adjacent donor. At this stage we have not been able to directly identify which specific absorption events (from 250 to 325 nm) are leading to luminescence.<sup>18</sup> To highlight the complicated nature of the calculated absorption profile in BrBFL–IPrCH<sub>2</sub> (**8**), selected transitions, corresponding to S<sub>1</sub>, S<sub>7</sub>, S<sub>8</sub>, and S<sub>9</sub> in Figure 7a, are presented (see Figure 9). We did note that the strong emission feature at 435 nm in each adduct (leading to blue luminescence) was absent when the BrBFL–LB compounds were irradiated at longer wavelengths in the range of 285–305 nm. Thus, the high-energy absorptions centered at 250 nm are leading to blue light emission; in addition, the same long-wavelength excitation led to the retention of the minor intensity emission band at 315–325 nm for compounds **2**, **5**, **8**, and **12**. In each case, irradiation at a longer wavelength (450 nm) did not yield any discernible luminescence. Lastly, the Cy<sub>3</sub>P adduct BrBFL–PCy<sub>3</sub> (**6**) was prepared to see if donor-based  $\pi^*$  orbitals were directly involved in luminescence. Compound **6** gave similar emission data as the corresponding IPr, IPrCH<sub>2</sub>, and PPh<sub>3</sub> adducts, lending added support for the exclusive participation of the borafluorene unit in emission; however, excitation could involve the occupation of ligand-based S<sub>n</sub> ( $n > 1$ ) excited states that decay nonradiatively to lower emissive states.

The absorption spectrum for the DMAP adduct [(DMAP)<sub>2</sub>BFL]Br (**7**) was also evaluated computationally by TD-DFT, with good agreement between the experimental and computational data (see Supporting Information, Figure S11).<sup>18</sup> Because of a relatively lower number of electronic transitions in **7**, a more detailed analysis could be conducted. Two major absorptions near 280 nm were identified by TD-DFT, and in each band, contributions from DMAP ( $\pi$  to  $\pi^*$ ) localized transitions are mixed with borafluorene ( $\pi$ ) to DMAP ( $\pi^*$ ) electronic transitions and states involving orbital population from both fragments. In addition, some contribution associated with borafluorene-localized  $\pi$ – $\pi^*$  transitions are present; however, as with compounds **5** and **8**, a clear path toward emission cannot be discerned at this time.

## CONCLUSIONS

A series of complexes featuring electron-deficient borafluorene units was prepared and comprehensively characterized. Specifically bright blue luminescence was noted in BrBFL–IPr (**2**), BrBFL–PPh<sub>3</sub> (**5**), BrBFL–PCy<sub>3</sub> (**6**), [(DMAP)<sub>2</sub>BFL]Br (**7**), and XBFL–IPrCH<sub>2</sub> (X = Br and H; **8** and **12**), with quantum efficiencies as high as 63% noted. Furthermore, computational studies (TD-DFT) were used to analyze the electronic transitions available to these species, and the invariant nature of the emission profiles in the series BrBFL–LB suggests that the borafluorene unit is largely responsible for the observed luminescence. This study is significant as it involves the syntheses of a new class of well-defined tetravalent organoborane emitter, and future work will be geared toward modifying the anionic substituent at boron (by replacing Br

Table 1. Crystallographic Data for Compounds 2, 3, and 7–9

	2-CH <sub>2</sub> Cl <sub>2</sub>	3	7·1/3 CH <sub>2</sub> Cl <sub>2</sub> ·1/2 THF	8·2 CH <sub>2</sub> Cl <sub>2</sub>	9·2 CH <sub>2</sub> Cl <sub>2</sub>
formula	C <sub>40</sub> H <sub>46</sub> BBBr Cl <sub>2</sub> N <sub>2</sub>	C <sub>39</sub> H <sub>43</sub> BN <sub>2</sub>	C <sub>28.33</sub> H <sub>32.67</sub> BBBr Cl <sub>0.67</sub> N <sub>4</sub> O <sub>0.5</sub>	C <sub>42</sub> H <sub>50</sub> BBBr Cl <sub>4</sub> N <sub>2</sub>	C <sub>30</sub> H <sub>43</sub> Br Cl <sub>4</sub> N <sub>2</sub>
formula wt	716.41	552.58	551.60	815.36	653.37
cryst. dimens. (mm)	0.41 × 0.24 × 0.23	0.45 × 0.42 × 0.35	0.30 × 0.26 × 0.18	0.36 × 0.14 × 0.11	0.31 × 0.13 × 0.07
cryst. syst.	monoclinic	monoclinic	monoclinic	monoclinic	triclinic
space group	P2 <sub>1</sub> /c	P2 <sub>1</sub> /n	C2/c	P2 <sub>1</sub> /n	P $\bar{1}$
unit cell					
a (Å)	11.4012 (4)	11.3096 (4)	29.9685 (7)	12.5593 (9)	11.6745 (3)
b (Å)	21.2295 (8)	14.8357 (6)	12.7445 (3)	22.5211 (15)	12.1104 (3)
c (Å)	15.8472 (6)	20.1829 (8)	43.8064 (10)	15.1550 (10)	12.2440 (3)
α (°)					79.3360 (10)
β (°)		104.2470 (10)	91.3286 (4)	101.145 (3)	85.4340 (10)
γ (°)					89.7850 (10)
V (Å <sup>3</sup> )	103.6023 (5)	3282.3 (2)	16726.6 (7)	4205.7 (5)	1695.69 (7)
Z	4	4	24	4	2
ρ <sub>calcd</sub> (g cm <sup>-3</sup> )	1.276	1.118	1.314	1.288	1.280
μ (mm <sup>-1</sup> )	1.276	0.064	1.564	3.895	4.698
T (K)	173(1)	173(1)	173(1)	173(1)	173(1)
2θ <sub>max</sub> (°)	52.82	52.80	52.95	140.43	136.70
total data	29 726	26 087	66 493	27 177	11 375
unique data (R <sub>int</sub> )	7649 (0.0406)	6735 (0.0214)	17236 (0.0370)	7844 (0.0217)	5928 (0.0125)
observed data [I > 2σ(I)]	6154	5571	11962	7335	5299
params.	415	383	897	452	362
R <sub>1</sub> [I > 2σ(I)] <sup>a</sup>	0.0374	0.0400	0.0659	0.0350	0.0419
wR <sub>2</sub> [all data] <sup>a</sup>	0.0940	0.1090	0.1996	0.0914	0.1166
difference map, Δρ (e Å <sup>-3</sup> )	0.782/−0.886	0.217/−0.183	1.510/−1.198	0.877/−0.625	0.674/−0.533

$$^a R_1 = \frac{\sum ||F_o| - |F_c||}{\sum |F_o|}; wR_2 = \left[ \frac{\sum w(F_o^2 - F_c^2)^2}{\sum w(F_o^4)} \right]^{1/2}$$

with a variety of nucleophiles) to develop new air-stable materials for OLED technologies.<sup>1</sup>

## EXPERIMENTAL SECTION

**General.** Author: All reactions were performed using standard Schlenk line techniques under an atmosphere of nitrogen or in an inert atmosphere glovebox (MBraun Inc.). Solvents were dried using a Grubbs-type solvent purification system<sup>25</sup> manufactured by Innovative Technology Inc., degassed (freeze–pump–thaw method), and stored over molecular sieves under a nitrogen atmosphere prior to use. Boron tribromide (1.0 M solution in hexanes), allylmagnesium bromide (1.0 M solution in diethyl ether), *n*-butyllithium (*n*-BuLi, 2.5 M solution in hexanes), *N,N*-dimethylaminopyridine (DMAP), Li[AlH<sub>4</sub>], K[N(SiMe<sub>3</sub>)<sub>2</sub>], Ag[OTf], PPh<sub>3</sub>, and Cy<sub>3</sub>P were obtained from Aldrich and used as received. 1,2-Dibromobenzene was purchased from Matrix Scientific and used as received. Hydrogen bromide gas was purchased from Matheson Gas Products Canada and used as received. [Rh(COD)Cl]<sub>2</sub> was purchased from Strem Chemicals, Inc. and used as received. 1,3-Bis-(2,6-diisopropylphenyl)-imidazol-2-ylidene (IPr),<sup>26</sup> 1,3-bis-(2,6-diisopropylphenyl)-2-methyleneimidazoline (IPrCH<sub>2</sub>),<sup>15a</sup> and 2,2'-dibromobiphenyl<sup>27</sup> were prepared following literature procedures. <sup>11</sup>B{<sup>1</sup>H}, <sup>11</sup>B, <sup>19</sup>F{<sup>1</sup>H}, and <sup>31</sup>P NMR spectra were recorded on a Varian iNova-500 spectrometer referenced externally to F<sub>3</sub>B–OEt<sub>2</sub> (<sup>11</sup>B), CFCl<sub>3</sub> (<sup>19</sup>F{<sup>1</sup>H}), and 85% H<sub>3</sub>PO<sub>4</sub> (<sup>31</sup>P), respectively. <sup>1</sup>H, <sup>1</sup>H{<sup>11</sup>B}, and <sup>13</sup>C{<sup>1</sup>H} NMR spectra were recorded on a Varian VNMR5-500 spectrometer and referenced externally to SiMe<sub>4</sub>. Elemental analyses were performed by the Analytical and Instrumentation Laboratory at the University of Alberta. Mass spectra were obtained on an Agilent 6220 spectrometer. Melting points were measured in a sealed glass capillary under nitrogen using a Meltemp melting point apparatus and are uncorrected. UV/vis spectra were obtained from a Cary 400 UV/vis spectrometer. Photoluminescence spectra were obtained from a Photon Technology International (PTI) MP1 Fluorescence System. The quantum yield of [(DMAP)<sub>2</sub>BFI]Br (7) was measured relative to naphthalene in cyclohexane, assuming a quantum yield (Φ) of 0.23;<sup>28a</sup> the quantum yields for the remaining

adducts were measured relative to quinine sulfate in 1 N H<sub>2</sub>SO<sub>4</sub> (Φ = 0.55).<sup>28b</sup>

**X-ray Crystallography.** Crystals of suitable quality for X-ray crystallography were removed from a vial in a glovebox and coated immediately with a thin layer of hydrocarbon oil (Paratone-N). A suitable crystal was picked and mounted on a glass fiber and then quickly placed in a low-temperature stream of nitrogen on the X-ray diffractometer.<sup>29</sup> All data were collected using a Bruker APEX II CCD detector/D8 diffractometer with Mo Kα radiation or Cu Kα radiation, with crystals cooled to −100 °C. The data were corrected for absorption<sup>30</sup> through Gaussian integration [BrBFI–IPr (2), [IPrMe]Br (9), BrBFI–IPrCH<sub>2</sub> (8)] or multiscan SADABS<sup>31</sup> (HBFI–IPr (3)) from the indexing of the crystal faces. Structures were solved using direct methods SHELXD ([IPrMe]Br (9)), SHELXS-97 (HBFI–IPr (3), BrBFI–IPrCH<sub>2</sub> (8)), intrinsic phasing SHELXT<sup>32</sup> ([[(DMAP)<sub>2</sub>BFI]Br (7)], or Patterson/structure expansion facilities within the DIRDIF-2008<sup>33</sup> program suite (BrBFI–IPr (2)) and refined using SHELXS-97.<sup>32</sup> Hydrogen atoms were assigned positions based on the sp<sup>2</sup> or sp<sup>3</sup> hybridization geometries of their attached carbon atoms and were given thermal parameters 20% greater than those of their parent atoms. Table 1 contains selected X-ray crystallographic data for each of the reported compounds.

**Special Refinement Conditions.** *Compound 7.* Attempts to refine peaks of residual electron density as disordered or partial-occupancy solvent tetrahydrofuran oxygen or carbon atoms were unsuccessful. The data were corrected for disordered electron density through use of the SQUEEZE procedure<sup>34</sup> as implemented in PLATON.<sup>35</sup> A total solvent-accessible void volume of 2100.4 Å<sup>3</sup> with a total electron count of 448 (consistent with 12 molecules of solvent THF, or one-half THF molecule per formula unit of 7, found in the unit cell. Restraints were applied to distances involving the disordered 4-dimethylaminopyridine group: d(N3C–C41C) = d(N3C–C45C) = d(N3D–C41D) = d(N3D–C45D) = 1.36(1) Å; d(N3C–B1C) = d(N3D–B1C) = 1.59(1) Å; d(N4C–C46C) = d(N4C–C47C) = d(N4D–C46D) = d(N4D–C47D) = 1.45(1) Å; d(C41C–C42C) = d(C44C–C45C) = d(C41D–C42D) = d(C44D–C45D) = 1.36(1) Å; d(C42C–C43C) = d(C43C–C44C) =



$d(\text{C42D}-\text{C43D}) = d(\text{C43D}-\text{C44D}) = 1.41(1) \text{ \AA}$ . Distances within the disordered solvent  $\text{CH}_2\text{Cl}_2$  molecule were restrained during refinement:  $d(\text{Cl1S}-\text{Cl1S}) = d(\text{Cl2S}-\text{Cl1S}) = d(\text{Cl3S}-\text{C2S}) = d(\text{Cl4S}-\text{C2S}) = 1.75(1) \text{ \AA}$ ;  $d(\text{Cl1S}-\text{---Cl2S}) = d(\text{Cl3S}-\text{---Cl4S}) = 2.85(1) \text{ \AA}$ .

**Compound 12.** The C–Cl distances (C2S–Cl3S, C2S–Cl4S, C3S–Cl5S, C3S–Cl6S) within the disordered dichloromethane solvent molecule were restrained to be the same.

**Theoretical Studies.** All calculations were carried out using the Gaussian 09 software package at the B3LYP/6-31G(d,p) level of theory.<sup>36</sup> Implicit solvent effects were taken into account by using the integral equation formalism version of the polarizable continuum model (IEF-PCM) for dichloromethane.<sup>37</sup> If available, crystal structures were used as input geometries. Default convergence criteria were chosen for the geometry optimizations. The obtained optimized geometries were confirmed to be local energy minimum structures by performing vibrational frequency analysis. For the calculation of the vertical excitation spectra using TD-DFT, nonequilibrium state-specific solvation of the excited states were accounted for. The reported transition wavelengths were shifted by ca. 25 nm to higher wavelengths than the calculated values. The electronic absorbance spectra were then obtained by assigning a uniform Gaussian band shape of 0.3 eV half-width at  $1/e^-$  height. The molecular orbitals were extracted from the output using GaussView 5 and assuming an isovalue of 0.02.

## SYNTHETIC PROCEDURES

**Synthesis of 9-Bromo-9-borofluorene (BrBFI, 1).** A solution of 2,2'-dibromobiphenyl (3.140 g, 10.06 mmol) in toluene (50 mL) was prepared and sparged with  $\text{N}_2$ . The solution was then cooled to  $-78^\circ\text{C}$ , and *n*-BuLi (14.0 mL, 22 mmol, 1.6 M solution in hexanes) was added dropwise. The resulting mixture was allowed to slowly warm to room temperature and stirred for 48 h. The mixture was then cooled to  $-78^\circ\text{C}$  before a solution of  $\text{BBr}_3$  (11.0 mL, 11 mmol, 1.0 M solution in hexanes) was added dropwise. The resulting mixture was allowed to slowly warm to room temperature and stirred for 12 h. The supernatant was decanted, and the remaining precipitate was extracted with  $3 \times 50$  mL of toluene; the toluene extracts were combined with the initial supernatant before the volatile components were then removed in vacuo. The crude product was recrystallized from hexanes at  $-35^\circ\text{C}$  to afford the product **1** as yellow needles (2.208 g, 90%).

$^1\text{H NMR}$  ( $\text{CDCl}_3$ , 500 MHz):  $\delta$  7.56 (d,  $^3J_{\text{HH}} = 7.2$  Hz, 2H, ArH), 7.37 (td,  $^3J_{\text{HH}} = 7.6$  Hz,  $^4J_{\text{HH}} = 1.2$  Hz, 2H, ArH), 7.33 (d,  $^3J_{\text{HH}} = 7.0$  Hz, 2H, ArH), 7.15 (td,  $^3J_{\text{HH}} = 7.0$  Hz,  $^4J_{\text{HH}} = 1.2$  Hz, 2H, ArH).  $^{13}\text{C}\{^1\text{H}\}$  NMR ( $\text{CDCl}_3$ , 125 MHz):  $\delta$  152.9 (ArC), 135.5 (ArC), 133.4 (ArC), 128.7 (ArC), 119.7 (ArC).  $^{11}\text{B}\{^1\text{H}\}$  NMR ( $\text{CDCl}_3$ , 160 MHz):  $\delta$  65.8 (s).<sup>6</sup>

**Synthesis of BrBFI–IPr (2).** To a mixture of compound **1** (503.9 mg, 2.074 mmol) and IPr (804.4 mg, 2.070 mmol) was added 20 mL of toluene. The mixture was allowed to stir for 12 h, during which time a colorless precipitate formed. The supernatant was decanted, the remaining solid was washed with  $3 \times 20$  mL of toluene, and the insoluble solid was dried under vacuum to afford product **2** as a white powder (1.218 g, 93%). Crystals suitable for X-ray analysis were grown from a 50/50 mixture of dichloromethane and hexanes at  $-35^\circ\text{C}$ .

$^1\text{H NMR}$  ( $\text{C}_6\text{D}_6$ , 500 MHz):  $\delta$  7.43 (d,  $^3J_{\text{HH}} = 7.6$  Hz, 2H, ArH), 7.25 (t,  $^3J_{\text{HH}} = 7.6$  Hz, 2H, ArH), 7.01 (d,  $^3J_{\text{HH}} = 7.6$  Hz, 4H, ArH), 6.97 (td,  $^3J_{\text{HH}} = 7.6$  Hz,  $^4J_{\text{HH}} = 1.2$  Hz, 2H, ArH), 6.57 (td,  $^3J_{\text{HH}} = 7.6$  Hz,  $^4J_{\text{HH}} = 1.2$  Hz, 2H, ArH), 6.40 (d,  $^3J_{\text{HH}} = 7.2$  Hz, 2H, ArH), 6.28 (s, 2H, –N–CH–), 2.79 (septet,  $^3J_{\text{HH}} = 6.8$  Hz, 4H,  $\text{CH}(\text{CH}_3)_2$ ), 1.08 (d,  $^3J_{\text{HH}} = 6.4$  Hz, 12H,  $\text{CH}(\text{CH}_3)_2$ ), 0.90 (d,  $^3J_{\text{HH}} = 7.2$  Hz, 12H,  $\text{CH}(\text{CH}_3)_2$ ).

$^{13}\text{C}\{^1\text{H}\}$  NMR ( $\text{C}_6\text{D}_6$ , 125 MHz):  $\delta$  149.7 (ArC), 146.2 (ArC), 136.1 (ArC), 134.3 (ArC), 131.1 (ArC), 129.1 (ArC), 126.5 (ArC), 125.1 (ArC), 124.8 (ArC), 118.7 (–N–CH–), 30.2 ( $\text{CH}(\text{CH}_3)_2$ ), 29.3 ( $\text{CH}(\text{CH}_3)_2$ ), 26.0 ( $\text{CH}(\text{CH}_3)_2$ ), 22.2 ( $\text{CH}(\text{CH}_3)_2$ ).  $^{11}\text{B}\{^1\text{H}\}$  NMR ( $\text{C}_6\text{D}_6$ , 160 MHz):  $\delta$  –6.4 (s). UV/vis (in  $\text{CH}_2\text{Cl}_2$ ):  $\lambda_{\text{max}} = 272$  nm ( $\epsilon = 5.3 \times 10^3 \text{ L mol}^{-1} \text{ cm}^{-1}$ ). Luminescence emission (in  $\text{CH}_2\text{Cl}_2$ ):  $\lambda_{\text{em}} = 324, 435$  nm, luminescence quantum yield:  $\Phi = 0.19$ , relative to quinine sulfate in 1 N  $\text{H}_2\text{SO}_4$ . HR-MS EI (positive mode,  $m/z$ ): Calcd. for  $[\text{M}-\text{Br}]^+$ : 551.35974. Found: 551.35892 ( $\Delta\text{ppm} = 1.5$ ). Anal. Calcd. for  $\text{C}_{39}\text{H}_{44}\text{BBrN}_2$ : C, 74.18; H, 7.02; N, 4.44. Found: C, 73.53; H, 7.17; N, 4.28%. Mp ( $^\circ\text{C}$ ): no melting or decomposition up to 340.

**Synthesis of HBFI–IPr (3).** To a mixture of compound **2** (102.2 mg, 0.162 mmol) and  $\text{Li}[\text{AlH}_4]$  (24.5 mg, 0.646 mmol) was added 15 mL of toluene. The resulting mixture was allowed to stir for 5 days. The mixture was then filtered through a small (ca. 1 cm) plug of silica gel. The volatile components were removed from the filtrate in vacuo, and the remaining crude solid was washed with 5 mL of diethyl ether to yield product **3** as a white solid (24.2 mg, 27%). Crystals suitable for X-ray analysis were grown from a 50/50 mixture of dichloromethane and hexanes at  $-35^\circ\text{C}$ .

$^1\text{H NMR}$  ( $\text{CDCl}_3$ , 500 MHz):  $\delta$  7.34 (d,  $^3J_{\text{HH}} = 6.5$  Hz, 2H, ArH), 7.28 (d,  $^3J_{\text{HH}} = 7.5$  Hz, 2H, ArH), 7.23 (d,  $^3J_{\text{HH}} = 6.0$  Hz, 4H, ArH), 7.10 (s, 2H, –N–CH–), 7.08 (d,  $^3J_{\text{HH}} = 8.0$  Hz, 4H, ArH), 6.94 (td,  $^3J_{\text{HH}} = 7.5$  Hz,  $^4J_{\text{HH}} = 1.5$  Hz, 2H, ArH), 6.90 (td,  $^3J_{\text{HH}} = 7.5$  Hz,  $^4J_{\text{HH}} = 1.5$  Hz, 2H, ArH), 2.81 (septet,  $^3J_{\text{HH}} = 7.0$  Hz, 4H,  $\text{CH}(\text{CH}_3)_2$ ), 1.17 (d,  $^3J_{\text{HH}} = 7.0$  Hz, 12H,  $\text{CH}(\text{CH}_3)_2$ ), 1.11 (d,  $^3J_{\text{HH}} = 6.5$  Hz, 12H,  $\text{CH}(\text{CH}_3)_2$ ).  $^{13}\text{C}\{^1\text{H}\}$  NMR ( $\text{CDCl}_3$ , 125 MHz):  $\delta$  149.2 (ArC), 145.2 (ArC), 134.2 (ArC), 131.4 (ArC), 130.1 (ArC), 124.9 (ArC), 124.1 (ArC), 123.5 (ArC), 118.4 (–N–CH–), 29.8 ( $\text{CH}(\text{CH}_3)_2$ ), 29.0 ( $\text{CH}(\text{CH}_3)_2$ ), 26.4 ( $\text{CH}(\text{CH}_3)_2$ ), 22.3 ( $\text{CH}(\text{CH}_3)_2$ ).  $^{11}\text{B}\{^1\text{H}\}$  NMR ( $\text{CDCl}_3$ , 160 MHz):  $\delta$  –19.1 (s).  $^{11}\text{B}$  NMR ( $\text{CDCl}_3$ , 160 MHz):  $\delta$  –19.1 (d,  $^1J_{\text{BH}} = 84$  Hz). HR-MS EI (positive mode,  $m/z$ ): Calcd. for  $[\text{M}]^+$ : 552.36755. Found: 552.36558 ( $\Delta\text{ppm} = 3.6$ ). Anal. Calcd. for  $\text{C}_{39}\text{H}_{45}\text{BBrN}_2$ : C, 84.77; H, 8.21; N, 5.07. Found: C, 84.77; H, 8.30; N, 5.13%. Mp ( $^\circ\text{C}$ ): 308–310.

**Synthesis of [BFI–IPr]OTf (4).** To a mixture of compound **2** (500.1 mg, 0.792 mmol) and  $\text{Ag}[\text{OTf}]$  (203.1 mg, 0.791 mmol) was added 15 mL of  $\text{CH}_2\text{Cl}_2$ . The reaction mixture was protected from light and allowed to stir for 12 h. The resulting mixture was filtered and all volatiles were removed from the filtrate in vacuo to afford the crude product as a pale yellow solid. The crude product was recrystallized from 10 mL of a 50/50 mixture of dichloromethane/hexanes at  $-35^\circ\text{C}$  to afford product **4** as a colorless solid (250.9 mg, 45%).

$^1\text{H NMR}$  ( $\text{CDCl}_3$ , 500 MHz):  $\delta$  7.35 (t,  $^3J_{\text{HH}} = 7.6$  Hz, 2H, ArH), 7.27 (d,  $^3J_{\text{HH}} = 6.8$  Hz, 2H, ArH), 7.15 (d,  $^3J_{\text{HH}} = 7.6$  Hz, 2H, ArH), 7.11 (s, 2H, –N–CH–), 7.10 (d,  $^3J_{\text{HH}} = 7.6$  Hz, 4H, ArH), 7.02 (td,  $^3J_{\text{HH}} = 7.2$  Hz,  $^4J_{\text{HH}} = 1.2$  Hz, 2H, ArH), 6.96 (td,  $^3J_{\text{HH}} = 7.2$  Hz,  $^4J_{\text{HH}} = 1.2$  Hz, 2H, ArH), 2.68 (septet,  $^3J_{\text{HH}} = 6.8$  Hz, 4H,  $\text{CH}(\text{CH}_3)_2$ ), 1.22 (d,  $^3J_{\text{HH}} = 6.8$  Hz, 12H,  $\text{CH}(\text{CH}_3)_2$ ), 1.09 (d,  $^3J_{\text{HH}} = 6.8$  Hz, 12H,  $\text{CH}(\text{CH}_3)_2$ ).  $^{13}\text{C}\{^1\text{H}\}$  NMR ( $\text{CDCl}_3$ , 125 MHz):  $\delta$  150.0 (ArC), 144.6 (ArC), 134.0 (ArC), 131.0 (ArC), 130.7 (ArC), 127.9 (ArC), 126.5 (ArC), 125.4 (ArC), 123.8 (ArC), 119.0 (–N–CH–), 29.8 ( $\text{CH}(\text{CH}_3)_2$ ), 29.2 ( $\text{CH}(\text{CH}_3)_2$ ), 26.6 ( $\text{CH}(\text{CH}_3)_2$ ), 22.0 ( $\text{CH}(\text{CH}_3)_2$ ).  $^{11}\text{B}\{^1\text{H}\}$  NMR ( $\text{CDCl}_3$ , 160 MHz):  $\delta$  2.3 (s).  $^{19}\text{F}\{^1\text{H}\}$  NMR ( $\text{CDCl}_3$ , 376 MHz):  $\delta$  –77.8 (s). HR-MS EI

(positive mode,  $m/z$ ): Calcd. for  $[M]^+$ : 700.31177. Found: 700.31221 ( $\Delta\text{ppm} = 0.6$ ). Anal. Calcd. for  $\text{C}_{40}\text{H}_{44}\text{BF}_3\text{N}_2\text{O}_3\text{S}$ : C, 68.57; H, 6.33; N, 4.00. Found: C, 68.35; H, 6.43; N, 4.03%. Mp ( $^\circ\text{C}$ ): 312 (decomposition).

**Synthesis of BrBFI–PPh<sub>3</sub> (5).** To a mixture of compound **1** (93.1 mg, 0.383 mmol) and PPh<sub>3</sub> (100.0 mg, 0.381 mmol) was added 15 mL of toluene. The resulting mixture was allowed to stir for 12 h. All volatile components were removed in vacuo and the remaining solid was washed with 10 mL of hexanes and dried before the product **5** was isolated as a white solid (176.7 mg, 92%).

<sup>1</sup>H NMR (CDCl<sub>3</sub>, 500 MHz):  $\delta$  7.57 (dd, <sup>3</sup>J<sub>HP</sub> = 9.2 Hz, <sup>3</sup>J<sub>HH</sub> = 7.5 Hz, 6H, ArH in PPh<sub>3</sub>), 7.49 (td, <sup>3</sup>J<sub>HH</sub> = 7.0 Hz, <sup>4</sup>J<sub>HH</sub> = 1.5 Hz, 2H, ArH), 7.42 (d, <sup>3</sup>J<sub>HH</sub> = 7.5 Hz, 2H, ArH), 7.37–7.32 (m, 9H, ArH in PPh<sub>3</sub>), 7.14 (tt, <sup>3</sup>J<sub>HH</sub> = 7.5 Hz, <sup>4</sup>J<sub>HH</sub> = 1.0 Hz, 2H, ArH), 6.99 (td, <sup>3</sup>J<sub>HH</sub> = 7.0 Hz, <sup>4</sup>J<sub>HH</sub> = 1.0 Hz, 2H, ArH). <sup>13</sup>C{<sup>1</sup>H} NMR (CDCl<sub>3</sub>, 125 MHz):  $\delta$  148.8 (d, <sup>3</sup>J<sub>CP</sub> = 7.0 Hz, ArC), 134.2 (d, <sup>3</sup>J<sub>CP</sub> = 8.2 Hz, ArC), 132.2 (d, <sup>5</sup>J<sub>CP</sub> = 1.8 Hz, ArC), 131.8 (d, <sup>4</sup>J<sub>CP</sub> = 2.5 Hz, ArC), 128.6 (d, <sup>2</sup>J<sub>CP</sub> = 10.3 Hz, ArC), 127.8 (d, <sup>4</sup>J<sub>CP</sub> = 2.0 Hz, ArC), 126.5 (d, <sup>4</sup>J<sub>CP</sub> = 2.3 Hz, ArC), 125.4 (d, <sup>1</sup>J<sub>CP</sub> = 59.3 Hz, ArC), 119.4 (s, ArC). <sup>11</sup>B{<sup>1</sup>H} NMR (CDCl<sub>3</sub>, 160 MHz):  $\delta$  –7.4 (s). <sup>31</sup>P{<sup>1</sup>H} NMR (CDCl<sub>3</sub>, 202 MHz):  $\delta$  1.8 (s). UV/vis (in CH<sub>2</sub>Cl<sub>2</sub>):  $\lambda_{\text{max}}$  = 248 nm ( $\epsilon = 2.30 \times 10^4 \text{ L mol}^{-1} \text{ cm}^{-1}$ ), 254 nm ( $\epsilon = 2.64 \times 10^4 \text{ L mol}^{-1} \text{ cm}^{-1}$ ). Luminescence emission (in CH<sub>2</sub>Cl<sub>2</sub>):  $\lambda_{\text{em}}$  = 315, 435 nm, luminescence quantum yield:  $\Phi = 0.50$ , relative to quinine sulfate in 1 N H<sub>2</sub>SO<sub>4</sub>. HR-MS EI (positive mode,  $m/z$ , %): 262.0909 (M<sup>+</sup> – BrBFI, 100), 184.0411 (Ph<sub>2</sub>P<sup>+</sup>, 9), 183.0363 (Ph<sub>2</sub>P<sup>+</sup> – H, 51), 152.0627 (Ph<sub>2</sub><sup>2+</sup>, 9), 108.0128 (PhP<sup>+</sup>, 25), 91.0548 (BrB<sup>+</sup>, 3), 77.0389 (Ph<sup>+</sup>, 4). Anal. Calcd. for C<sub>30</sub>H<sub>23</sub>BBRP: C, 71.32; H, 4.59. Found: C, 72.18; H, 4.81%. Mp ( $^\circ\text{C}$ ): 209–212.

**Synthesis of BrBFI–PCy<sub>3</sub> (6).** To a mixture of compound **1** (0.161 g, 0.663 mmol) and PCy<sub>3</sub> (0.186 g, 0.663 mmol) was added 10 mL of toluene. The resulting mixture was allowed to stir for 2 h. The solution was decanted, and the remaining solid was washed with toluene (3  $\times$  10 mL) and dried before compound **6** was isolated as a white solid (0.301 g, 87%). <sup>1</sup>H NMR (CDCl<sub>3</sub>, 500 MHz): 7.49 (dd, <sup>3</sup>J<sub>HH</sub> = 7.0 Hz, ArH), 7.42 (d, <sup>3</sup>J<sub>HH</sub> = 7.5 Hz, 2H, ArH), 7.14 (tt, <sup>3</sup>J<sub>HH</sub> = 7.5 Hz, <sup>4</sup>J<sub>HH</sub> = 1.0 Hz, 2H, ArH), 6.99 (td, <sup>3</sup>J<sub>HH</sub> = 7.0 Hz, <sup>4</sup>J<sub>HH</sub> = 1.0 Hz, 2H, ArH), 2.30 (m, 3H, PCy<sub>3</sub>), 2.07 (s, 6H, PCy<sub>3</sub>), 1.76 (s, 3H, PCy<sub>3</sub>), 1.68 (d,  $J = 10.0$  Hz, 6H, PCy<sub>3</sub>), 1.17 (m, 15H, PCy<sub>3</sub>). <sup>13</sup>C{<sup>1</sup>H} NMR (CDCl<sub>3</sub>, 125 MHz):  $\delta$  148.2 (s, ArC), 132.2 (s, ArC), 127.6 (s, ArC), 126.5 (s, ArC), 119.7 (s, ArC), 32.3 (d, CyC), 28.2 (s, CyC), 27.4 (s, CyC), 25.9 (s, CyC). <sup>11</sup>B{<sup>1</sup>H} NMR (CDCl<sub>3</sub>, 160 MHz):  $\delta$  –6.8 (s). <sup>31</sup>P{<sup>1</sup>H} NMR (CDCl<sub>3</sub>, 202 MHz):  $\delta$  –1.3 (s). UV/vis (in CH<sub>2</sub>Cl<sub>2</sub>):  $\lambda_{\text{max}}$  = 254 nm ( $\epsilon = 2.30 \times 10^4 \text{ L mol}^{-1} \text{ cm}^{-1}$ ). Luminescence emission (in CH<sub>2</sub>Cl<sub>2</sub>):  $\lambda_{\text{em}}$  = 316 nm, 435 nm, luminescence quantum yield:  $\Phi = 0.31$ , relative to quinine sulfate in 1 N H<sub>2</sub>SO<sub>4</sub>. Anal. Calcd. for C<sub>30</sub>H<sub>41</sub>BBrP: C, 68.85; H, 7.90. Found: C, 69.18; H, 7.81%. Mp ( $^\circ\text{C}$ ): 225–226.

**Synthesis of [(DMAP)<sub>2</sub>BFI]Br (7).** To a mixture of compound **1** (199.4 mg, 0.821 mmol) and *N,N*-dimethylaminopyridine (DMAP, 202.8 mg, 1.660 mmol) was added 15 mL of toluene. The resulting mixture was allowed to stir for 12 h. The supernatant was decanted, and the remaining solid was washed with 15 mL of toluene and dried in vacuo to afford compound **7** as a white solid (354.3 mg, 89%). Crystals suitable for X-ray analysis were grown from a 50/50 mixture of CH<sub>2</sub>Cl<sub>2</sub> and THF at –35  $^\circ\text{C}$ .

<sup>1</sup>H NMR (CDCl<sub>3</sub>, 500 MHz):  $\delta$  8.05 (m, 4H, ArH in DMAP), 7.64 (dt, <sup>3</sup>J<sub>HH</sub> = 7.5 Hz, <sup>4</sup>J<sub>HH</sub> = 0.5 Hz, 2H, ArH), 7.49 (dt, <sup>3</sup>J<sub>HH</sub> = 7.5 Hz, <sup>4</sup>J<sub>HH</sub> = 0.5 Hz, 2H, ArH), 7.31 (td, <sup>3</sup>J<sub>HH</sub> = 7.5 Hz, <sup>4</sup>J<sub>HH</sub> = 1.0 Hz, 2H, ArH), 7.20 (td, <sup>3</sup>J<sub>HH</sub> = 7.5 Hz, <sup>4</sup>J<sub>HH</sub> = 1.0 Hz, 2H, ArH), 6.80 (m, 4H, ArH in DMAP), 3.16 (s, 12H, N(CH<sub>3</sub>)<sub>2</sub> in DMAP). <sup>13</sup>C{<sup>1</sup>H} NMR (CDCl<sub>3</sub>, 125 MHz):  $\delta$  156.3 (ArC), 149.2 (ArC), 143.4 (ArC), 130.2 (ArC), 128.9 (ArC), 128.2 (ArC), 127.5 (ArC), 125.3 (ArC), 120.0 (ArC), 40.1 (N(CH<sub>3</sub>)<sub>2</sub>). <sup>11</sup>B{<sup>1</sup>H} NMR (CDCl<sub>3</sub>, 160 MHz):  $\delta$  4.6 (s). UV/vis (in CH<sub>2</sub>Cl<sub>2</sub>):  $\lambda_{\text{max}}$  = 320 nm ( $\epsilon = 1.85 \times 10^4 \text{ L mol}^{-1} \text{ cm}^{-1}$ ). Luminescence emission (in CH<sub>2</sub>Cl<sub>2</sub>):  $\lambda_{\text{em}}$  = 355 nm, luminescence quantum yield:  $\Phi = 0.42$ , relative to naphthalene in cyclohexane. HR-MS ES (positive mode,  $m/z$ ): [M–Br]<sup>+</sup>; 407.2399. Anal. Calcd. for C<sub>26</sub>H<sub>28</sub>BBRN<sub>4</sub>: C, 64.09; H, 5.79; N, 11.50. Found: C, 65.30; H, 5.81; N, 10.31%. Mp ( $^\circ\text{C}$ ): 144–147.

**Synthesis of BrBFI–IPrCH<sub>2</sub> (8).** To a mixture of compound **1** (504.5 mg, 2.08 mmol) and IPrCH<sub>2</sub> (412.7 mg, 1.03 mmol) was added 20 mL of toluene. The mixture was allowed to stir for 72 h, during which time a colorless precipitate formed. The supernatant was decanted, and the remaining solid was washed with 3  $\times$  15 mL of toluene. All volatile components were removed from the solid in vacuo to afford compound **8** as a white powder (638.5 mg, 96%). Crystals suitable for X-ray analysis were grown from a 50/50 mixture of dichloromethane and hexanes at –35  $^\circ\text{C}$ .

<sup>1</sup>H NMR (CDCl<sub>3</sub>, 500 MHz):  $\delta$  7.68 (t, <sup>3</sup>J<sub>HH</sub> = 8.0 Hz, 2H, ArH), 7.50 (d, <sup>3</sup>J<sub>HH</sub> = 8.0 Hz, 4H, ArH), 7.36 (d, <sup>3</sup>J<sub>HH</sub> = 7.5 Hz, 2H, ArH), 7.22 (s, 2H, –N–CH–), 6.95 (td, <sup>3</sup>J<sub>HH</sub> = 7.0 Hz, <sup>4</sup>J<sub>HH</sub> = 1.5 Hz, 2H, ArH), 6.69 (td, <sup>3</sup>J<sub>HH</sub> = 7.0 Hz, <sup>4</sup>J<sub>HH</sub> = 1.5 Hz, 2H, ArH), 5.94 (d, <sup>3</sup>J<sub>HH</sub> = 9.0 Hz, 2H, ArH), 3.05 (septet, <sup>3</sup>J<sub>HH</sub> = 7.0 Hz, 4H, CH(CH<sub>3</sub>)<sub>2</sub>), 2.66 (s, 2H, –CH<sub>2</sub>–B), 1.34 (d, <sup>3</sup>J<sub>HH</sub> = 6.5 Hz, 12H, CH(CH<sub>3</sub>)<sub>2</sub>), 1.37 (d, <sup>3</sup>J<sub>HH</sub> = 7.0 Hz, 12H, CH(CH<sub>3</sub>)<sub>2</sub>). <sup>13</sup>C{<sup>1</sup>H} NMR (CDCl<sub>3</sub>, 125 MHz):  $\delta$  160.5 (ArC), 146.7 (ArC), 146.1 (ArC), 131.6 (ArC), 131.5 (ArC), 129.3 (ArC), 126.1 (ArC), 125.8 (ArC), 125.7 (ArC), 122.1 (ArC), 118.5 (–N–CH–), 29.2 (–CH<sub>2</sub>–B), 26.4 (CH(CH<sub>3</sub>)<sub>2</sub>), 22.9 (CH(CH<sub>3</sub>)<sub>2</sub>). <sup>11</sup>B{<sup>1</sup>H} NMR (CDCl<sub>3</sub>, 160 MHz):  $\delta$  –1.4 (s). UV/vis (in CH<sub>2</sub>Cl<sub>2</sub>):  $\lambda_{\text{max}}$  = 248 nm ( $\epsilon = 2.84 \times 10^4 \text{ L mol}^{-1} \text{ cm}^{-1}$ ), 254 nm ( $\epsilon = 2.91 \times 10^4 \text{ L mol}^{-1} \text{ cm}^{-1}$ ). Luminescence emission (in CH<sub>2</sub>Cl<sub>2</sub>):  $\lambda_{\text{em}}$  = 320, 435 nm, luminescence quantum yield:  $\Phi = 0.63$ , relative to quinine sulfate in 1 N H<sub>2</sub>SO<sub>4</sub>. HR-MS EI (positive mode,  $m/z$ ): Calcd. for [BrBFI]<sup>+</sup>: 243.98819. Found: 243.98620 ( $\Delta\text{ppm} = 8.2$ ). Calcd. for [IPrCH<sub>2</sub>]<sup>+</sup>: 402.30350. Found: 402.30281 ( $\Delta\text{ppm} = 1.7$ ). Anal. Calcd. for C<sub>40</sub>H<sub>46</sub>BBRN<sub>2</sub>: C, 74.42; H, 7.18; N, 4.34. Found: C, 73.15; H, 7.05; N, 4.20%. Mp ( $^\circ\text{C}$ ): 228–231.

**Synthesis of [IPrMe]Br (9).** Gaseous HBr was bubbled through a solution of IPrCH<sub>2</sub> (100.2 mg, 0.249 mmol) in 10 mL of toluene until a colorless precipitate formed (approximately 30 s). The resulting precipitate was isolated by filtration and dried in vacuo to give compound **9** as a white solid (115.3 mg, 96%).

<sup>1</sup>H NMR (CDCl<sub>3</sub>, 500 MHz):  $\delta$  8.15 (s, 2H, –N–CH–), 7.62 (t, <sup>3</sup>J<sub>HH</sub> = 7.5 Hz, 2H, ArH), 7.39 (d, <sup>3</sup>J<sub>HH</sub> = 7.5 Hz, 4H, ArH), 2.28 (septet, <sup>3</sup>J<sub>HH</sub> = 7.0 Hz, 4H, CH(CH<sub>3</sub>)<sub>2</sub>), 2.08 (s, 3H, –CH<sub>3</sub>), 1.28 (d, <sup>3</sup>J<sub>HH</sub> = 7.0 Hz, 12H, CH(CH<sub>3</sub>)<sub>2</sub>), 1.18 (d, <sup>3</sup>J<sub>HH</sub> = 7.0 Hz, 12H, CH(CH<sub>3</sub>)<sub>2</sub>). <sup>13</sup>C{<sup>1</sup>H} NMR (CDCl<sub>3</sub>, 125 MHz):  $\delta$  145.0 (N–C–N), 144.9 (ArC), 132.6 (ArC), 129.1 (ArC), 126.8 (ArC), 125.4 (–N–CH–), 29.2 (CH(CH<sub>3</sub>)<sub>2</sub>), 24.8 (CH(CH<sub>3</sub>)<sub>2</sub>), 23.5 (CH(CH<sub>3</sub>)<sub>2</sub>), 11.0 (–CH<sub>3</sub>). HR-MS EI (positive mode,  $m/z$ ): Calcd. for [IPrMe]<sup>+</sup>: 403.3108. Found:

403.3101 ( $\Delta\text{ppm} = 1.6$ ). Anal. Calcd. for  $\text{C}_{28}\text{H}_{39}\text{BrN}_2$ : C, 69.55; H, 8.13; N, 5.79. Found: C, 70.46; H, 7.80; N, 4.92%. Mp ( $^{\circ}\text{C}$ ): 225 (decomposition).

**Synthesis of  $(\text{Me}_3\text{Si})_2\text{NBFI}$  (11).** To a solution of compound **1** (45.5 mg, 0.187 mmol) in 5 mL of toluene was added a solution of  $\text{K}[\text{N}(\text{SiMe}_3)_2]$  (32.9 mg, 0.165 mmol) in 5 mL of toluene. The resulting mixture was allowed to stir overnight before being filtered. The volatile components were removed in vacuo to afford compound **11** as a red semisolid (40.6 mg, 76%).

$^1\text{H}$  NMR ( $\text{CDCl}_3$ , 500 MHz):  $\delta$  7.63 (dt,  $^3J_{\text{HH}} = 7.2$  Hz,  $^4J_{\text{HH}} = 1.2$  Hz, 2H, ArH), 7.44 (dt,  $^3J_{\text{HH}} = 7.2$  Hz,  $^4J_{\text{HH}} = 1.2$  Hz, 2H, ArH), 7.30 (td,  $^3J_{\text{HH}} = 7.6$  Hz,  $^4J_{\text{HH}} = 1.2$  Hz, 2H, ArH), 7.14 (td,  $^3J_{\text{HH}} = 7.6$  Hz,  $^4J_{\text{HH}} = 1.2$  Hz, 2H, ArH), 0.37 (s, 18H, Si- $\text{CH}_3$ ).  $^{13}\text{C}\{^1\text{H}\}$  NMR ( $\text{CDCl}_3$ , 125 MHz):  $\delta$  152.6 (ArC), 133.1 (ArC), 132.0 (ArC), 127.4 (ArC), 119.2 (ArC), 4.6 (Si- $\text{CH}_3$ ).  $^{11}\text{B}\{^1\text{H}\}$  NMR ( $\text{CDCl}_3$ , 160 MHz):  $\delta$  54.2 (s).  $^{29}\text{Si}\{^1\text{H}\}$  NMR ( $\text{CDCl}_3$ , 100 MHz):  $\delta$  3.4 (s). See the Supporting Information for copies of the NMR spectra.<sup>18</sup>

**Synthesis of  $\text{HBFI-IPrCH}_2$  (12).** To a mixture of compound **8** (202.2 mg, 0.313 mmol) and  $\text{Li}[\text{AlH}_4]$  (25.7 mg, 0.677 mmol) was added 10 mL of  $\text{CH}_2\text{Cl}_2$ . The resulting mixture was allowed to stir for 5 days. The mixture was then filtered through a small (ca. 1 cm) plug of silica gel. The volatile components were removed from the filtrate in vacuo to yield compound **12** as a white solid (152.4 mg, 86%).

$^1\text{H}\{^{11}\text{B}\}$  NMR ( $\text{CDCl}_3$ , 500 MHz):  $\delta$  7.64 (t,  $^3J_{\text{HH}} = 8.0$  Hz, 2H, ArH), 7.49 (d,  $^3J_{\text{HH}} = 7.5$  Hz, 2H, ArH), 7.43 (d,  $^3J_{\text{HH}} = 8.0$  Hz, 4H, ArH), 7.08 (s, 2H, -N-CH-), 6.94 (td,  $^3J_{\text{HH}} = 7.5$  Hz,  $^4J_{\text{HH}} = 1.0$  Hz, 2H, ArH), 6.73 (td,  $^3J_{\text{HH}} = 7.5$  Hz,  $^4J_{\text{HH}} = 1.0$  Hz, 2H, ArH), 6.12 (d,  $^3J_{\text{HH}} = 7.0$  Hz, 2H, ArH) 2.77 (septet,  $^3J_{\text{HH}} = 7.0$  Hz, 4H, CH( $\text{CH}_3$ )<sub>2</sub>), 2.35 (broad, 1H, -BH, assignment made by broadband  $^1\text{H}\{^{11}\text{B}\}$  decoupling), 2.15 (d,  $^3J_{\text{HH}} = 3.5$  Hz, 2H, -CH<sub>2</sub>-B) 1.25 (d,  $^3J_{\text{HH}} = 7.0$  Hz, 12H, CH( $\text{CH}_3$ )<sub>2</sub>), 1.21 (d,  $^3J_{\text{HH}} = 6.5$  Hz, 12H, CH( $\text{CH}_3$ )<sub>2</sub>).  $^{13}\text{C}\{^1\text{H}\}$  NMR ( $\text{CDCl}_3$ , 125 MHz):  $\delta$  163.5 (ArC), 148.1 (ArC), 145.8 (ArC), 131.6 (ArC), 131.3 (ArC), 130.1 (ArC), 125.2 (ArC), 124.3 (ArC), 123.5 (ArC), 121.5 (ArC), 118.2 (-N-CH-), 29.2 (CH( $\text{CH}_3$ )<sub>2</sub>), 25.8 (CH( $\text{CH}_3$ )<sub>2</sub>), 22.6 (CH( $\text{CH}_3$ )<sub>2</sub>).  $^{11}\text{B}\{^1\text{H}\}$  NMR ( $\text{CDCl}_3$ , 160 MHz):  $\delta$  -15.1 (s).  $^{11}\text{B}$  NMR ( $\text{CDCl}_3$ , 160 MHz):  $\delta$  -15.1 (d,  $^1J_{\text{BH}} = 82$  Hz). UV/vis (in  $\text{CH}_2\text{Cl}_2$ ):  $\lambda_{\text{max}} = 315$  nm ( $\epsilon = 8.64 \times 10^3$  L mol<sup>-1</sup> cm<sup>-1</sup>). Luminescence emission (in  $\text{CH}_2\text{Cl}_2$ ):  $\lambda_{\text{em}} = 324, 435$  nm, luminescence quantum yield:  $\Phi = 0.19$ , relative to quinine sulfate in 1 N  $\text{H}_2\text{SO}_4$ . HR-MS EI (positive mode,  $m/z$ ): Calcd. for  $[\text{M}]^+$ : 566.38324. Found: 566.38218 ( $\Delta\text{ppm} = 1.9$ ). Anal. Calcd. for  $\text{C}_{40}\text{H}_{47}\text{BN}_2$ : C, 84.79; H, 8.36; N, 4.94. Found: C, 79.65; H, 8.04; N, 4.56%. Mp ( $^{\circ}\text{C}$ ): 218–220. Despite repeated attempts, combustion analysis gave consistently low values for carbon content (lower by ca. 5%). See the Supporting Information for copies of the NMR spectra.<sup>18</sup>

**Decomposition of Compound 12 in THF and  $\text{CH}_2\text{Cl}_2$ .** Note that compound **12** is prone to decomposition in THF and in  $\text{CH}_2\text{Cl}_2$  in the absence of  $\text{Li}[\text{AlH}_4]$ .

A solution of 27.4 mg (0.048 mmol) of compound **12** in 10 mL of THF was prepared and allowed to stir for 3 days.  $^{11}\text{B}$  NMR spectroscopy revealed that  $\sim 70\%$  decomposition had occurred, and the emergence of three new boron environments were observed.  $^{11}\text{B}$  NMR ( $\text{C}_6\text{D}_6$ , 160 MHz):  $\delta$  3.3 (br, new environment), -6.1 (s, new environment), -14.5 (d,  $^1J_{\text{BH}} = 82$  Hz, **12**, ca. 30%) -19.1 (t,  $^1J_{\text{BH}} = 83$  Hz, new environment).

A solution of 29.6 mg (0.052 mmol) of compound **12** in 10 mL of  $\text{CH}_2\text{Cl}_2$  was prepared and allowed to stir for 3 days.  $^{11}\text{B}$

NMR spectroscopy revealed that  $\sim 70\%$  conversion to  $[\text{IPrMe}]\text{Cl}^{15\text{b}}$  had occurred and  $^{11}\text{B}$  NMR spectroscopy revealed two new boron environments.  $^{11}\text{B}$  NMR ( $\text{CDCl}_3$ , 160 MHz):  $\delta$  2.3 (br, new environment), -6.7 (s, new environment), -15.1 (d,  $^1J_{\text{BH}} = 82$  Hz, **12**, ca. 30%).

## ■ ASSOCIATED CONTENT

### 📄 Supporting Information

Includes crystallographic data for (IPrMe)Br, NMR spectra for compounds **11** and **12**, absorbance and fluorescence spectra for compounds **2**, **6**, **7**, and **12**, and calculated electronic transitions for compounds **5**, **7**, and **8**. This material is available free of charge via the Internet at <http://pubs.acs.org>.

## ■ AUTHOR INFORMATION

### ✉ Corresponding Author

\*Corresponding Author E-mail: [erivard@ualberta.ca](mailto:erivard@ualberta.ca).

### Notes

The authors declare no competing financial interest.

## ■ ACKNOWLEDGMENTS

This work was supported by the Natural Sciences and Engineering Research Council (NSERC) of Canada (Discovery Grant for E.R.), the Canada Foundation for Innovation (CFI), Alberta Innovates-Technologies Futures (New Faculty Award to E.R.), and Suncor Energy Inc. (Petro-Canada Young Innovator Award to E.R.). C.M. acknowledges the Alexander von Humboldt foundation for a Feodor Lynen Postdoctoral Fellowship. We also gratefully acknowledge access to the computing facilities provided by the Western Canada Research Grid (Westgrid). We also thank Wayne Moffat for his assistance in collecting luminescence and quantum yield data.

## ■ REFERENCES

- (1) (a) Loudet, A.; Burgess, K. *Chem. Rev.* **2007**, *107*, 4891. (b) Boens, N.; Leen, V.; Dehaen, W. *Chem. Soc. Rev.* **2012**, *41*, 1130. (c) Rao, Y.-L.; Wang, S. *Inorg. Chem.* **2011**, *50*, 12263. (d) Zhou, Z.; Wakamiya, A.; Kushida, T.; Yamaguchi, S. *J. Am. Chem. Soc.* **2012**, *134*, 4529. (e) Zhao, C.-H.; Wakamiya, A.; Inukai, Y.; Yamaguchi, S. *J. Am. Chem. Soc.* **2006**, *128*, 15934. (f) Jäkle, F. *Chem. Rev.* **2010**, *110*, 3985. (g) Jaska, C. A.; Emslie, D. J. H.; Bosdet, M. J. D.; Piers, W. E.; Sorensen, T. S.; Parvez, M. *J. Am. Chem. Soc.* **2006**, *128*, 10885. (h) Mercier, L. G.; Piers, W. E.; Parvez, M. *Angew. Chem., Int. Ed.* **2009**, *48*, 6108.
- (2) (a) Reus, C.; Weidlich, S.; Bolte, M.; Lerner, H.-W.; Wagner, M. *J. Am. Chem. Soc.* **2013**, *135*, 12892. (b) Januszewski, E.; Bolte, M.; Lerner, H.-W.; Wagner, M. *Organometallics* **2012**, *31*, 8420. (c) Hoffend, C.; Diefenbach, M.; Januszewski, E.; Bolte, M.; Lerner, H.-W.; Holthausen, M. C.; Wagner, M. *Dalton Trans.* **2013**, *42*, 13826. (d) Hoffend, C.; Schödel, F.; Bolte, M.; Lerner, H.-W.; Wagner, M. *Chem.—Eur. J.* **2012**, *18*, 15394.
- (3) For related studies, see (a) Dou, C.; Saito, S.; Yamaguchi, S. *J. Am. Chem. Soc.* **2013**, *135*, 9346. (b) Mercier, L. G.; Piers, W. E.; Harrington, R. W.; Clegg, W. *Organometallics* **2013**, *32*, 6820. (c) Wood, T. K.; Piers, W. E.; Keay, B. A.; Parvez, M. *Angew. Chem., Int. Ed.* **2009**, *48*, 4009.
- (4) Yamaguchi, S.; Shirasaka, T.; Akiyama, S.; Tamao, K. *J. Am. Chem. Soc.* **2002**, *124*, 8816.
- (5) (a) Chen, P.; Jäkle, F. *J. Am. Chem. Soc.* **2011**, *133*, 20142. (b) Kuhtz, M.; Cheng, F.; Schwedler, S.; Böhlting, L.; Brockhinke, A.; Weber, L.; Parab, K.; Jäkle, F. *ACS Macro Lett.* **2012**, *1*, 555. (c) Cheng, F.; Bonder, E. M.; Salem, S.; Jäkle, F. *Macromolecules* **2013**, *46*, 2905. (d) Parab, K.; Doshi, A.; Cheng, F.; Jäkle, F. *Macromolecules* **2011**, *44*, 5961.
- (6) Narula, C. K.; Nöth, H. *J. Organomet. Chem.* **1985**, *281*, 131.

- (7) Hübner, A.; Lerner, H.-W.; Wagner, M.; Bolte, M. *Acta Crystallogr.* **2010**, E66, o444.
- (8) (a) Braunschweig, H.; Chiu, C.-W.; Damme, A.; Ferkinghoff, K.; Kraft, K.; Radacki, K.; Wahler, J. *Organometallics* **2011**, *30*, 3210. (b) Braunschweig, H.; Chiu, C.-W.; Radacki, K.; Kupfer, T. *Angew. Chem., Int. Ed.* **2010**, *49*, 2041.
- (9) (a) Das, A.; Hübner, A.; Weber, M.; Bolte, M.; Lerner, H.-W.; Wagner, M. *Chem. Commun.* **2011**, 47, 11339. (b) Hübner, A.; Diefenbach, M.; Bolte, M.; Lerner, H.-W.; Holthausen, M. C.; Wagner, M. *Angew. Chem., Int. Ed.* **2012**, *51*, 12514. (c) Breunig, J. M.; Hübner, A.; Bolte, M.; Wagner, M.; Lerner, H.-W. *Organometallics* **2013**, *32*, 6792. (d) Hübner, A.; Qu, Z.-W.; Englert, U.; Bolte, M.; Lerner, H.-W.; Holthausen, M. C.; Wagner, M. *J. Am. Chem. Soc.* **2011**, *133*, 4596.
- (10) (a) Matsumoto, T.; Gabbai, F. P. *Organometallics* **2009**, *28*, 4252. For reviews on cationic boron species, see (b) Kölle, P.; Nöth, H. *Chem. Rev.* **1985**, *85*, 399. (c) Piers, W. E.; Bourke, S. C.; Conroy, K. D. *Angew. Chem., Int. Ed.* **2005**, *44*, 5016.
- (11) Boersma, D. A.; Goff, H. M. *Inorg. Chem.* **1982**, *21*, 581.
- (12) (a) Hudnall, T. W.; Gabbai, F. P. *Chem. Commun.* **2008**, 4596. (b) Bonnier, C.; Piers, W. E.; Parvez, M.; Sorensen, T. S. *Chem. Commun.* **2008**, 4593.
- (13) Narula, C. K.; Nöth, H. *Inorg. Chem.* **1985**, *24*, 2532.
- (14) Biswas, S.; Oppel, I. M.; Bettinger, H. F. *Inorg. Chem.* **2010**, *49*, 4499.
- (15) (a) Al-Rafia, S. M. I.; Malcolm, A. C.; Liew, S. K.; Ferguson, M. J.; McDonald, R.; Rivard, E. *Chem. Commun.* **2011**, 47, 6987. (b) Al-Rafia, S. M. I.; Ferguson, M. J.; Rivard, E. *Inorg. Chem.* **2011**, *50*, 10543. (c) Malcolm, A. C.; Sabourin, K. J.; McDonald, R.; Ferguson, M. J.; Rivard, E. *Inorg. Chem.* **2012**, *51*, 12905. (d) Al-Rafia, S. M. I.; Momeni, M. R.; McDonald, R.; Ferguson, M. J.; Brown, A.; Rivard, E. *Angew. Chem., Int. Ed.* **2013**, *52*, 6390. (e) Al-Rafia, S. M. I.; Momeni, M. R.; Ferguson, M. J.; McDonald, R.; Brown, A.; Rivard, E. *Organometallics* **2013**, *32*, 6658. For recent reviews covering Lewis base–borane adducts, see (f) Staubitz, A.; Robertson, A. P. M.; Sloan, M. E.; Manners, I. *Chem. Rev.* **2010**, *110*, 4023. (g) Curran, D. P.; Solov'yev, A.; Brahma, M. M.; Fensterbank, L.; Malacria, M.; Lacôte, E. *Angew. Chem., Int. Ed.* **2011**, *50*, 10294.
- (16) (a) Dumrath, A.; Wu, X. -F.; Neumann, H.; Spannenberg, A.; Jackstell, R.; Beller, M. *Angew. Chem., Int. Ed.* **2010**, *49*, 8988. (b) Wang, Y.; Abraham, M. Y.; Gillard, R. J.; Sexton, D. R.; Wei, P.; Robinson, G. H. *Organometallics* **2013**, *32*, 6639. (c) Wang, Y. -B.; Wang, Y. -M.; Zhang, W. -Z.; Lu, X. -B. *J. Am. Chem. Soc.* **2013**, *135*, 11996.
- (17) Kuhn, N.; Bohnen, H.; Kreutzberg, J.; Bläser, D.; Boese, R. J. *Chem. Soc., Chem. Commun.* **1993**, 1136.
- (18) See the Supporting Information for full details.
- (19) It was hoped that placing an electron-releasing IPr=CH group adjacent to an electron-withdrawing borafuorene unit in (IPr=CH)BFL (**10**) would lead to enhanced luminescence via a “push-pull” mechanism. (a) Coluccini, C.; Sharma, A. K.; Caricato, M.; Sironi, A.; Cariati, E.; Righetto, S.; Tordin, E.; Botta, C.; Forni, A.; Pasini, D. *Phys. Chem. Chem. Phys.* **2013**, *15*, 1666. (b) Weber, L.; Eickhoff, D.; Kahlert, J.; Böbling, L.; Brockhinke, A.; Stammler, H.-G.; Neumann, B.; Fox, M. A. *Dalton Trans.* **2012**, 41, 10328. (c) Achelle, S.; Barsella, A.; Baudequin, C.; Caro, B.; Robin-le Guen, F. *J. Org. Chem.* **2012**, *77*, 4087.
- (20) Al-Rafia, S. M. I.; Malcolm, A. C.; Liew, S. K.; Ferguson, M. J.; Rivard, E. *J. Am. Chem. Soc.* **2011**, *133*, 777.
- (21) Structural characterization of the possible borafuorene–DMF adduct, formulated herein as TripBFL–DMF, has not been reported; see reference 4.
- (22) The emission of the BrBFL–LB adducts remained unchanged in solution in the presence of a large excess of added bromide, in the form of [*n*-Bu<sub>4</sub>N]Br, indicating that the emission is not likely arising from a cationic borenium species [LB–BFL]<sup>+</sup>, although we cannot completely rule out this possibility at this stage.
- (23) (a) Umezawa, K.; Nakamura, Y.; Makino, H.; Citterio, D.; Suzuki, K. *J. Am. Chem. Soc.* **2008**, *130*, 1550. (b) Bonnier, C.; Piers, W. E.; Al-Sheikh Ali, A.; Thompson, A.; Parvez, M. *Organometallics* **2009**, *28*, 4845.
- (24) Allinger, N. L.; Siefert, J. H. *J. Am. Chem. Soc.* **1975**, *97*, 752.
- (25) Pangborn, A. B.; Giardello, M. A.; Grubbs, R. H.; Rosen, R. K.; Timmers, F. J. *Organometallics* **1996**, *15*, 1518.
- (26) Jafarpour, L. S.; Stevens, E. D.; Nolan, S. P. *J. Organomet. Chem.* **2000**, 606, 49.
- (27) Dougherty, T. K.; Lau, K. S. Y.; Hedberg, F. L. *J. Org. Chem.* **1983**, *48*, 5273.
- (28) (a) Brouwer, A. M. *Pure Appl. Chem.* **2011**, *83*, 2213. (b) Swager, T. M.; Gil, C. J.; Wrighton, M. S. *J. Phys. Chem.* **1995**, *99*, 4886.
- (29) Hope, H. *Prog. Inorg. Chem.* **1995**, 43, 1.
- (30) Blessing, R. H. *Acta Crystallogr.* **1995**, A51, 33.
- (31) Sheldrick, G. M. *SADABS, Version 2008/1*; Universität Göttingen: Göttingen, Germany, 2008.
- (32) Sheldrick, G. M. *Acta Crystallogr.* **2008**, A64, 112.
- (33) Beurskens, P. T.; Beurskens, G.; de Gelder, R.; Smits, J. M. M.; Garcia-Granda, S.; Gould, R. O. *DIRDIF—2008*; Crystallography Laboratory, Radboud University: Nijmegen, The Netherlands, 2008.
- (34) van der Sluis, P. S.; Spek, A. L. *Acta Crystallogr.* **1990**, A46, 194.
- (35) *PLATON—A Multipurpose Crystallographic Tool*; Utrecht University: Utrecht, The Netherlands.
- (36) Frisch, M. J.; Trucks, G. W.; Schlegel, H. B.; Scuseria, G. E.; Robb, M. A.; Cheeseman, J. R.; Scalmani, G.; Barone, V.; Mennucci, B.; Petersson, G. A.; Nakatsuji, H.; Caricato, M.; Li, X.; Hratchian, H. P.; Izmaylov, A. F.; Bloino, J.; Zheng, G.; Sonnenberg, J. L.; Hada, M.; Ehara, M.; Toyota, K.; Fukuda, R.; Hasegawa, J.; Ishida, M.; Nakajima, T.; Honda, Y.; Kitao, O.; Nakai, H.; Vreven, T.; J. A. Montgomery, J.; Peralta, J. E.; Ogliaro, F.; Bearpark, M.; Heyd, J. J.; Brothers, E.; Kudin, K. N.; Staroverov, V. N.; Keith, T.; Kobayashi, R.; Normand, J.; Raghavachari, K.; Rendell, A.; Burant, J. C.; Iyengar, S. S.; Tomasi, J.; Cossi, M.; Rega, N.; Millam, J. M.; Klene, M.; Knox, J. E.; Cross, J. B.; Bakken, V.; Adamo, C.; Jaramillo, J.; Gomperts, R.; Stratmann, R. E.; Yazyev, O.; Austin, A. J.; Cammi, R.; Pomelli, C.; Ochterski, J. W.; Martin, R. L.; Morokuma, K.; Zakrzewski, V. G.; Voth, G. A.; Salvador, P.; Dannenberg, J. J.; Dapprich, S.; Daniels, A. D.; Farkas, O.; Foresman, J. B.; Ortiz, J. V.; Cioslowski, J.; Fox, D. J. *Gaussian 09*; Gaussian, Inc.: Wallingford, CT, 2010.
- (37) Tomasi, J.; Mennucci, B.; Cammi, R. *Chem. Rev.* **2005**, *105*, 2999.